

1 **Describing posterior distributions of variance components:**

2 **Problems and the use of null distributions to aid interpretation**

3 Joel L. Pick<sup>1,2,3,12,\*</sup>, Claudia Kasper<sup>4</sup>, Hassen Allegue<sup>5,12</sup>, Niels J. Dingemanse<sup>6,12</sup>, Ned  
4 A. Dochtermann<sup>7,12</sup>, Kate L. Laskowski<sup>8,12</sup>, Marcos R. Lima<sup>9,12</sup>, Holger Schielzeth<sup>10,12</sup>,  
5 David F. Westneat<sup>11,12</sup>, Jonathan Wright<sup>1,12</sup>, Yimen G. Araya-Ajoy<sup>1,3,12</sup>

6 <sup>1</sup> Centre for Biodiversity Dynamics (CBD), Department of Biology, Norwegian University  
7 of Science and Technology (NTNU), N-7491 Trondheim, Norway.

8 <sup>2</sup> Institute of Ecology and Evolution, University of Edinburgh, Charlotte Auerbach Road,  
9 Edinburgh, EH9 3FL, UK

10 <sup>3</sup> Both authors contributed equally

11 <sup>4</sup> Animal GenoPhenomics group, Agroscope, Tioleyre 4, CH-1725 Posieux, Switzerland.

12 <sup>5</sup> Département des Sciences Biologiques, Université du Québec à Montréal, Montréal,  
13 QC, Canada

14 <sup>6</sup> Behavioural Ecology, Department of Biology, Ludwig-Maximilians University of Mu-  
15 nich, Planegg-Martinsried, Germany

16 <sup>7</sup> Department of Biological Sciences, North Dakota State University, Fargo, ND, USA

17 <sup>8</sup> Department of Evolution and Ecology, University of California Davis, Davis, CA, USA

18 <sup>9</sup> Departamento de Biologia Animal e Vegetal, Centro de Ciências Biológicas, Universi-  
19 dade Estadual de Londrina, Londrina, Brazil

20 <sup>10</sup> Institute of Ecology and Evolution, Friedrich Schiller University Jena, Jena, Germany

21 <sup>11</sup> Department of Biology, University of Kentucky, Lexington, KY, USA

22 <sup>12</sup> Members of the SQuID working group

23 \* Corresponding author, email address: joel.l.pick@gmail.com

24 **Running title:** Null distributions for variance components

25 **Keywords:** hierarchical models, variance, null distribution, permutation, simulations,

26 squidSim

## 27 **Abstract**

28 1. Assessing the biological relevance of variance components estimated using MCMC-  
29 based mixed-effects models is not straightforward. Variance estimates are constrained  
30 to be greater than zero and their posterior distributions are often asymmetric. Different  
31 measures of central tendency for these distributions can therefore be very different, and  
32 credible intervals cannot overlap zero, making it difficult to assess the the size and statis-  
33 tical support for among-group variance. This is often done through visual inspection of  
34 the whole posterior distribution, and so relies on subjective decisions for interpretation.

35 2. We use simulations to demonstrate the difficulties of summarising the posterior  
36 distributions of variance estimates from MCMC-based models. We then describe different  
37 methods for generating the expected null distribution (i.e. a distribution of effect sizes  
38 that would be obtained if there was no among-group variance) that can be used to aid in  
39 the interpretation of variance estimates.

40 3. Through comparing commonly used summary statistics of posterior distributions of  
41 variance components, we showed that the posterior median is predominantly the least bi-  
42 ased. We further show how null distributions can be used to derive a p-value that provides  
43 complimentary information to the commonly presented measures of central tendency and  
44 uncertainty. Finally we show how these p-values can facilitates the implementation of  
45 power analyses within an MCMC framework.

46 4. The use of null distributions for variance components can aid study design and the  
47 interpretation of results from MCMC-based models. We hope that this manuscript will  
48 make empiricists using mixed models think more carefully about their results, what they  
49 present and what inference they can make.

## 50 Introduction

51 Estimating variance components using mixed-effects models is common in ecology and  
52 evolution (Bolker *et al.*, 2009; Harrison *et al.*, 2018). Mixed-effect models are a flexible  
53 statistical tool used to study hierarchically structured data, including extensions for esti-  
54 mating quantitative genetic parameters (animal models; Henderson, 1988; Kruuk, 2004)  
55 and comparative analysis (meta-analysis and phylogenetic mixed models; Hadfield & Nak-  
56 agawa, 2010). Markov chain Monte Carlo (MCMC) algorithms are increasingly used to  
57 fit mixed-effects models, due to their flexibility and availability of open-source software  
58 (e.g. winBUGS (Gilks *et al.*, 1994), JAGS (Plummer, 2003), MCMCglmm (Hadfield,  
59 2010), Stan (Stan Development Team, 2022b)). MCMC algorithms are a collection of  
60 probabilistic simulation methods for generating observations from designated statistical  
61 distributions and are typically implemented within a Bayesian framework (Gelman *et al.*,  
62 2013).

63 MCMC methods have many advantages in ecology and evolution. For instance, we are  
64 commonly interested in derived measures such as a standardised measure of variance (e.g.  
65 repeatability, heritability and evolvability Nakagawa & Schielzeth, 2010; Houle, 1992).  
66 These derived measures can be estimated using the whole posterior distribution of their  
67 components, allowing uncertainty to be propagated both within and among analyses. In  
68 contrast, in a maximum likelihood framework, the methods to estimate the uncertainty of  
69 derived metrics (such as the delta method) can be biased with small sample sizes (O’Hara  
70 *et al.*, 2008). Data in ecological and evolutionary studies are also commonly non-Gaussian,  
71 for example counts (e.g. number of offspring), binary and ratio data (e.g. survival,  
72 presence/absence, sex ratio) and categorical data (e.g. colour morphs, horn type in  
73 sheep). The performance of MCMC algorithms in generalized linear mixed-effects models  
74 has been found to be superior in terms of accuracy and precision compared with Restricted  
75 Maximum Likelihood (REML) approaches (O’Hara & Merilä, 2005; de Villemereuil *et al.*,  
76 2013). Bayesian methods also allow existing information to be incorporated as a prior

77 distribution, although this has rarely been used in ecological or evolutionary studies  
78 ([Lemoine, 2019](#)).

79 Despite these clear advantages, there are several issues that empiricists face when  
80 using MCMC mixed-effect models. Here we address the issue that variance estimates and  
81 their uncertainty can be hard to describe and interpret, especially when trying to assess  
82 their biological relevance. We highlight two problems that can occur when estimating  
83 variance components, both of which centre around the difficulty of describing the posterior  
84 distribution of variance components using summary statistics: (i) finding an appropriate  
85 measure of central tendency; and (ii) assessing the statistical support for non-zero among-  
86 group variance. These problems stem from variance estimates being constrained to be  
87 greater than zero and that their posterior distributions are often asymmetric.

88 In order to describe the posterior distribution, we often present some measure of cen-  
89 tral tendency alongside some measure of uncertainty (quantile-based intervals or Highest  
90 Posterior Density (HPD) intervals). The posterior mean, median and mode have all been  
91 used as measures of central tendency, and more recent works have suggested the general  
92 use of the posterior median ([Gelman \*et al.\*, 2020](#); [McElreath, 2020](#)). There is, however,  
93 no clear guidance on which measure provides a more appropriate summary statistic for  
94 variance components, although in our experience the mode and mean are most commonly  
95 reported. When the posterior distribution of a variance component is far away from zero  
96 and is symmetric, then the mean, median and mode are approximately equal (Figure  
97 [1a](#)) and inferences are robust to the choice of central tendency metric. However, when  
98 variances are small (relative to the total variance) and/or there are small sample sizes  
99 (both of which often occur in ecology and evolution), the posterior distributions can be  
100 close to zero. As variances are constrained to be greater than zero, these posterior dis-  
101 tributions are typically asymmetric and can even be bimodal. Consequently, there can  
102 be a considerable difference between the mean, median and mode, with the mode often  
103 lying close to zero (Figure [1b](#)). This discrepancy makes it is difficult to draw inference

104 about the magnitude of the posterior variance estimate.

105 Use of the posterior mode is often justified as being the closest to the maximum like-  
106 lihood estimate (MLE) when uninformative priors are used. However, this comparison  
107 refers to the joint posterior mode, rather than the marginal mode that is typically esti-  
108 mated and reported. In more complex models, the joint and marginal modes may differ  
109 (Held & Sabanés Bové, 2020, Section 6.5.4), meaning that the marginal mode and MLE  
110 are no longer the same. As shown in Figure S2, the convergence of the posterior mode  
111 and MLE also requires the use of uninformative improper priors, which are generally not  
112 advised (Gelman *et al.*, 2013) and are thus seldom used. The posterior mode is also hard  
113 to estimate; it is typically done using kernel density estimation and different methods  
114 may provide quite different estimates (Figure 2), thereby providing an additional source  
115 of hidden ambiguity. Furthermore, the mode requires a larger number of samples in  
116 the posterior distribution to be reliably estimated, and will show greater variation be-  
117 tween models/chains run on the same dataset (Kruschke, 2015). In contrast, the mean is  
118 strongly affected by extreme values, and so by the long tail of an asymmetric distribution.

119 It is also often important to assess statistical support for among-group variance at a  
120 particular level. Typically 95% credible intervals (CRIs) are presented as a measure of  
121 uncertainty in parameter estimates derived from MCMC model fits. As variance com-  
122 ponents cannot overlap zero, CRIs give no information about the compatibility of the  
123 estimates with the null hypothesis (no among-group variance). Posterior distributions  
124 are often inspected visually, as histograms or density plots, in order to assess whether the  
125 distributions are biased towards zero, which is commonly assumed to signify that the es-  
126 timated variance is not different from zero. What is seldom appreciated, however, is that  
127 the degree of smoothing that is applied in such plots (via the binning interval or band-  
128 width) can alter these conclusions. This means that the same distribution can be seen  
129 as uni- or bimodal, or peaking at zero or away from zero (Figure 2). Such assessments  
130 therefore tend to be highly subjective and lack a proper quantitative basis.

131 To address this, several methods for generating metrics for assessing the confidence  
132 in a result (such as p-values) have been suggested in a Bayesian framework (reviewed  
133 in [Makowski \*et al.\*, 2019a](#)). Two of these, Region of Practical Equivalence (ROPE) and  
134 Bayes factors, can be used for variance components. The ROPE approach identifies a  
135 range of values considered negligible or too small to be of any practical relevance (i.e. the  
136 Region of Practical Equivalence), and quantifies the proportion of overlap between the  
137 posterior distribution and the ROPE. This is similar to equivalence testing in a Frequen-  
138 tist framework, specifically to the two one-sided tests (TOST) approach ([Lakens \*et al.\*,  
139 2018](#)). Bayes factors are analogous to Frequentist likelihood ratios, comparing different  
140 models (for example with and without the random effects of interest), but unlike likeli-  
141 hood ratios they incorporate information from the prior distributions into the comparison  
142 of the models ([Morey \*et al.\*, 2016](#)). Both of these metrics can be used to provide a mea-  
143 sure of statistical support for estimates of variance components, but their implementation  
144 is complicated - ROPE requires the definition of a threshold, incorporating further sub-  
145 jectivity into the analysis, whilst the computation of Bayes factors can be challenging,  
146 and even not implementable in some commonly used programs (e.g. MCMCglmm). We  
147 discuss these two methods further in the discussion.

148 Here we suggest a complementary method to assess statistical support in mixed-effect  
149 models, which compares the estimated variance components to a null distribution in  
150 order to inform the statistical inferences made from the model. This involves creating a  
151 distribution of effect sizes that would be expected under the null hypothesis (no among-  
152 group variance) and comparing this null distribution with the observed among-group  
153 variance. This method has several advantages. Null distributions can be used to generate  
154 a p-value describing the probability that the observed estimate is as or more extreme than  
155 expected under the null hypothesis. Although often criticised through their association  
156 with Null Hypothesis Significance Testing (NHST; [Wasserstein & Lazar, 2016](#); [Amrhein  
157 \*et al.\*, 2017](#); [McShane \*et al.\*, 2019](#); [Amrhein \*et al.\*, 2019](#)), p-values have well understood  
158 and useful properties. When correctly interpreted, these test statistics provide a useful

159 tool by indicating how inconsistent an observed effect size is with a scenario in which  
160 there is no among-group variance. In contrast to the ROPE method, the creation of  
161 a null distribution requires no subjective decisions about thresholds and, in contrast to  
162 Bayes Factors, they can be implemented using the output from any Bayesian model.

163 We present two methods, permutation and simulation, for generating null distributions  
164 for variance components. When generating a null distribution using permutation, some  
165 feature of the data or data structure is randomised to produce a new dataset that contains  
166 the structure of the original dataset, but where there is no relationship between the  
167 response variable and the variable of interest (the among-group variance in this case).  
168 This randomization is repeated a large number of times (e.g. 1000) to create many  
169 different permuted datasets. The same analysis is then carried out on the permuted  
170 datasets as on the original dataset, and a test statistic of interest (e.g. the estimate of  
171 among-group variance) is used to create a null distribution of test statistics (Figure 1c,d).  
172 A (one-tailed) p-value can then be derived as the proportion of permuted datasets with  
173 a test statistic greater than or equal to the test statistic observed with the real data set.  
174 Permutation tests have already been suggested as an alternative to likelihood ratio tests  
175 for frequentist analyses (Fitzmaurice *et al.*, 2007; Samuh *et al.*, 2012), although they are  
176 not commonly utilized in ecology and evolution (but see Araya-Ajoy & Dingemanse, 2017;  
177 Stoffel *et al.*, 2017). Permutation tests are a subclass of nonparametric tests (Pesarin  
178 & Salmaso, 2010; Lehmann & Romano, 2005) and do not rely on specific probability  
179 distributions, and so make few assumptions. However, as we show later in the manuscript,  
180 datasets can be permuted in several different ways when the data structure is complex,  
181 and the consequences of the choices involved in such cases are often not immediately  
182 obvious. An alternative method of creating a null distribution is using simulations. This  
183 process is similar to permutation, but instead of generating permuted datasets we can  
184 simulate datasets from the observed model parameters (in a similar way to parametric  
185 bootstrapping), whilst setting the variance in question to zero. This simulation method  
186 makes more assumptions about the data and model, but allows for more control of the

187 manipulated features of the simulated datasets compared with permutations.

188 Finally, a crucial part of designing experiments and statistical analyses is assessing  
189 the power to detect an effect size of interest. Power is defined as the probability of  
190 rejecting the null hypothesis (i.e. no among-group variance) for a given effect size at  
191 a specified alpha level (typically 0.05), and so is dependent upon the generation of p-  
192 values. Although power relates to NHST and the often criticized alpha level ([Wasserstein](#)  
193 [& Lazar, 2016](#); [Amrhein \*et al.\*, 2017](#); [McShane \*et al.\*, 2019](#); [Amrhein \*et al.\*, 2019](#)), it  
194 and analogous metrics ([Gelman & Carlin, 2014](#)) remain an important tool for study  
195 design regardless of statistical philosophy, and this is because it provides a quantitative  
196 approach to calculating optimal sample sizes and designing sampling regimes. Power may  
197 also provide a more useful metric than precision when considering variance components.  
198 As their distributions are bounded at zero, standard errors will always decrease when  
199 distributions are close to zero (see Supplementary Figure S4). However, the concept  
200 of power for variance components in MCMC models is not well developed. As null  
201 distributions can be used to generate p-values, they also provide a convenient way of  
202 conducting power analysis.

203 Here, we first compare commonly used summary statistics of posterior distributions  
204 of variance components. We then demonstrate the utility of null distributions (i.e. a  
205 distribution of effect sizes that would be obtained if there was no among-group variance)  
206 to generate a complementary p-value statistic and aid the interpretation of the variance  
207 components. Comparison with a null distribution provides a quantitative measure of  
208 confidence that the observed variance component is larger than what might be expected  
209 under the null hypothesis, given the data structure and priors used. Importantly, we  
210 are not advocating that this approach should replace the presentation and use of ef-  
211 fect sizes (e.g. posterior mean/median/mode) and credible intervals, but rather that it  
212 should be used as an additional and complementary statistic. Finally, we show how null  
213 distributions can be used to perform a power analysis within an MCMC framework.

## 214 **Methods**

### 215 **Generation of Simulated Datasets**

216 Simulated datasets were generated out in R (version 4.1.0 [R Core Team, 2022](#)) using  
217 the squidSim R package (version 0.1.0 [Pick, 2022](#)). We first simulated Gaussian data  
218 with one hierarchical level and varied the number of observations per group (2 and 4)  
219 and the number of groups (20, 40 and 80). We simulated a total variance of 1 and  
220 varied the among-group variance (0, 0.1, 0.2 and 0.4; since the total variance simulated  
221 was 1, these are also the respective intra-class correlations (ICCs)/repeatabilities). We  
222 simulated every combination of these parameters (24 parameters sets) and for each set we  
223 simulated 500 datasets. Power to detect among-group variance is known to be determined  
224 by effect size and sample size both within and among groups. We deliberately chose these  
225 parameter values and sample sizes to explore scenarios where power is low ([Dingemans &  
226 Dochtermann, 2013](#)) to understand the impact on posterior distributions. These sample  
227 sizes also correspond to typical experimental designs in behavioral ecology or life history  
228 data collected on wild populations ([Bell \*et al.\*, 2009](#)).

229 We analysed each simulated dataset with a linear mixed-effect model specifying group  
230 level random effects in a Bayesian framework, using Stan with the rstan package (version  
231 2.21.3 [Stan Development Team, 2022a](#)). We specified weakly informative priors on the  
232 among-group and residual standard deviations (half-Cauchy distribution with scale 2),  
233 and ran one chain for each model with 5000 iterations and a warm-up period of 2000  
234 iterations. Across the majority of models (95%) this ensured an effective sample size  
235 in the posterior distribution of the among group variance of  $>500$ . For comparison, we  
236 also ran REML models using the lmer function of the lme4 package (version 1.1-29 [Bates  
237 \*et al.\*, 2015](#)), the results of which are shown in the Supplementary Figure [S1](#).

238 As a demonstration that our findings hold with more complex data, we simulated  
239 Bernoulli data (binomial with one observation) with 80 groups and 4 observations per

240 group. Among-group effects were simulated from a Gaussian distribution on the latent  
241 scale, with among-group variances of 0 and 0.2. The latent scale response variable was  
242 then transformed using the inverse logit function to provide the probabilities, and sampled  
243 with a Bernoulli process. We simulated 100 datasets for each variance, and analysed the  
244 data as outlined above.

## 245 **Comparison of Posterior Distribution Summary Statistics**

246 From the posterior distributions of the among-group variances, we calculated the posterior  
247 mean, median and mode, and compared these estimates with the simulated values.

248 While calculating the mean and median of the posterior distribution is straightfor-  
249 ward, there are several ways of estimating the mode of the marginal posterior distribution,  
250 which involve some (hidden) assumptions. Commonly used functions in R include the  
251 `posterior.mode` function in the `MCMCglmm` package (Hadfield, 2010), the `Mode` func-  
252 tion in the `ggdist` package (Kay, 2022), and the `map_estimate` function of the `bayestestR`  
253 package (Makowski *et al.*, 2019b). Typically these functions estimate the mode by es-  
254 timating the parameter value at which the kernel density is maximised. Kernel density  
255 estimation essentially involves fitting a model to the distribution of posterior samples  
256 to estimate a density function. The maximum of this function (the estimated mode) is  
257 then calculated over a series of predicted values. One key parameter in kernel density  
258 estimation is the bandwidth, which essentially describes the amount of smoothing and  
259 is analogous to the number of breakpoints in a histogram (Figure 2). Common meth-  
260 ods generally scale bandwidth generated by specific algorithms. `MCMCglmm` scales the  
261 bandwidth generated by Silverman’s ‘rule of thumb’ algorithm (`nrd0`; eqn 3.31 in Sil-  
262 verman, 1986) by 0.1 (i.e. it is much less smoothed; Figure 2d). In contrast, `ggdist`  
263 and `bayestestR` use the default values of the `nrd0` and `SJ` algorithms (Sheather & Jones,  
264 1991), respectively (the default bandwidth of the `nrd0` algorithm is also used by `density`  
265 function in R; Figure 2a). The impact on the potential inferences caused by the choice

266 of scaling is demonstrated in Figure 2, with the degree of smoothing affecting where the  
267 posterior mode is estimated. To explore this impact of bandwidth, we estimated the  
268 posterior mode using these two bandwidth scalings (0.1 and 1). The kernel density was  
269 estimated using the SJ algorithm (Sheather & Jones, 1991), and the mode was estimated  
270 using 512 predicted values with a cut point at zero. These additional parameters all differ  
271 between commonly used functions, but have much smaller impacts upon the results than  
272 the bandwidth, and so we hold them constant here.

273 To ensure that our results, especially on the mode, were not driven by the choice of  
274 the prior, we ran additional models on a subset of the data (ICC=0.2, N groups=80,  
275 N within=2) with a half-Cauchy prior with scale 5 and 25, and uniform priors from 0  
276 to 5 and 0 to 25 on the among-group standard deviation. The half Cauchy prior has  
277 been recommend for variance components (Gelman, 2006) and is commonly used (note  
278 it is equivalent to the parameter expanded priors in MCMCglmm). For demonstration  
279 purposes, we also ran models in MCMCglmm specifying uninformative improper priors.  
280 Given the simplicity of these models, the posterior mode is expected to correspond to the  
281 REML estimate. The different parametrizations of the half Cauchy and uniform priors  
282 resulted in no difference in the results (Figure S2). As expected, using an uninformative  
283 improper prior led to a concordance between REML and posterior mode, although the  
284 strength of this similarity differed between the different methods used to estimate the  
285 mode (Figure S2).

286 To compare these different measures of central tendency, we calculated the bias as  
287  $\frac{1}{n} \sum \hat{\theta}_i - \theta$  (where  $\theta$  is the true simulated value,  $\hat{\theta}_i$  is the model estimate from  $i$ th simulation  
288 in a parameter set, and  $n$  is the number of simulations). For the non-zero effect sizes,  
289 we also calculated relative bias  $\frac{1}{n} \sum \frac{\hat{\theta}_i - \theta}{\theta}$  and absolute relative bias  $\frac{1}{n} \sum \frac{|\hat{\theta}_i - \theta|}{\theta}$ . We also  
290 calculated the precision as  $1/\sqrt{\frac{1}{n} \sum (\hat{\theta}_i - \bar{\theta})^2}$ , which we present in the Supplementary  
291 Figure S4.

## 292 **Creation of null distributions and p-values**

293 We created null distributions for each simulated dataset using two methods. First, we  
294 permuted the datasets by shuffling the group indices (IDs) to create 100 new datasets,  
295 each of which was analysed in the same way as the original dataset. From each permuted  
296 dataset, we extracted the same parameters (the estimates of central tendency in the  
297 posterior distribution of the among-group variance) as for models fitted to the original  
298 data and created the corresponding null distributions. Second, we used simulations to  
299 create the null distribution. To do this, we simulated datasets with no among-group  
300 variance. To ensure the same total variance we added the posteriors of the among-group  
301 and residual variances of the original model, and we used the median of the resulting  
302 distribution as our inputted value for the simulated residual variance in the null model.  
303 The choice of the median for this step should have little consequence, as this derived  
304 distribution will be estimated with much less uncertainty and so will be symmetric,  
305 meaning that the three measures of central tendency will be equivalent. Each simulated  
306 null dataset was analysed in the same way as the original dataset, and we extracted the  
307 same parameters to create the corresponding null distributions.

308 Although we recommend using a larger number of permutations/simulations to build  
309 up a null distribution in empirical studies (e.g. 1000), here we used 100 permutations and  
310 simulations to generate null distributions for these simulated datasets in order to reduce  
311 the computational burden (500 simulations for 4 variances, with 6 different sample sizes is  
312 12000 datasets, for each of which we performed 100 permutations and 100 simulations).  
313 We then calculated a p-value for each original dataset, as the proportion of estimates  
314 in the null distribution that were higher than the estimate from the original data. We  
315 calculated p-values using each central tendency measure, and these are compared in  
316 Figure S5.

## 317 Power analysis

318 Using the simulated datasets outlined above, we compared two ways by which power can  
319 be calculated. Power is defined as the probability of rejecting the null hypothesis (i.e. no  
320 among-group variance in this case) for a given effect size and data structure at a specified  
321 alpha level (typically 0.05). To do this, we calculated the proportion of datasets in which  
322 the p-value was below a nominal threshold of 0.05. It is worth noting that, although  
323 power has a superficial connection with NHST, power can also be seen as a description  
324 of the distribution of p-values expected for a given effect size and data structure. Other  
325 descriptions of this distribution (e.g. the mean) would be simple functions of the power.  
326 We therefore chose to present power as a description of the distribution of p-values as it  
327 is conceptually well understood and frequently used, rather than due to any philosophical  
328 alignment with NHST.

329 First, we estimated power using the p-values generated through comparison with the  
330 null distributions from both permutation and simulation approaches outlined above ('full'  
331 method). We were also able to calculate the false positive rate for this method (essentially  
332 the power when the simulated value is 0). Second, we used the model estimates from the  
333 simulated datasets with zero among-group variance for each data structure (combination  
334 of among- and within-group sample sizes) as a null distribution, against which the es-  
335 timates from simulated datasets with among-group variance could be tested ('reduced'  
336 method). This method of estimating power is similar to the simulation method of gen-  
337 erating null distributions, but involves generating one null distribution for *all* datasets  
338 with the same data structure, instead of null distribution for *each* dataset. It is therefore  
339 massively less computationally intensive for power analyses, because to explore power  
340 within the parameter space presented here it only required the running 12,000 models,  
341 rather than 1,212,000. It is not possible to calculate a false positive rate for this method,  
342 as this would involve comparing the null distribution with itself, and so the false positive  
343 rate would be 5%, by definition.

## 344 Results

### 345 Comparing summary statistics of the posterior distribution

346 When the simulated among-group variance was zero, all summary statistics were up-  
347 wardly biased to some extent (the posterior distribution cannot include 0; Figure 3a).  
348 Predictably, the posterior mean and median from datasets with zero variance were con-  
349 siderably more upwardly biased for small sample sizes, in contrast to the mode. The  
350 mean was the most biased as it is heavily influenced by the tail of the distribution. Con-  
351 sequently, this upward bias is stronger when the uncertainty is high (i.e. when the tail is  
352 large). Note, however, that this upward bias is also present in Frequentist analyses (see  
353 Figure S1), and is not just a feature of Bayesian analyses.

354 When the simulated among-group variance is non-zero, then the mean, median and  
355 mode all appeared to be consistent estimators, in that any bias occurred only at small  
356 sample and/or effect sizes. The posterior median generally converged on the simulated  
357 value at lower effect and sample sizes (Figure 3b), as compared with the posterior mean,  
358 which was upwardly biased, and the posterior mode that was biased towards zero (Figure  
359 3b).

360 When considering the absolute relative bias (Figure 3c), the mean and median show  
361 very similar levels of bias, with exception of the lowest sample and effect size combination  
362 where the mean was more biased. This suggests that although the mean is more likely to  
363 be upwardly biased, the magnitude of the bias is similar in the two measures. However,  
364 the mode is consistently more biased than the other measures (Figure 3c), although  
365 this bias disappears at higher sample and effect sizes. Following the example shown in  
366 Figure 2, the bias in the mode depends upon the bandwidth that was used, with higher  
367 smoothing showing less bias across the two bandwidths tested. We found similar patterns  
368 in our Bernoulli simulations (Figure 5a).

## 369 Performance of the null distributions

370 As expected, both permutation and simulation methods produced a uniform distribution  
371 of p-values when applied to datasets where the simulated among-group variance was zero  
372 (Figures 4). The distribution of p-values from both tests then shifts towards zero as the  
373 sample size and the magnitude of the variance increase (Figure 4). Similar patterns were  
374 found in the Bernoulli simulations (Figure 5b).

375 Importantly, although the mean, median and mode were often quite different in magni-  
376 tude (reflecting skew in the posterior distribution), the inference based upon the p-values  
377 did not differ between the different metrics. There were strong correlations between p-  
378 values estimated with the different metrics, with the exception of the mode estimated  
379 with less smoothing (see Figures S5 and S7). P-values were also strongly correlated  
380 between null distributions generated through simulation and permutation methods (see  
381 Figures S6 and S8).

## 382 Power analyses

383 When considering the full method of estimating power, both ways of generating null  
384 distributions (permutation and simulation) gave very similar results (Figure 6), with  
385 marginally higher power for the permutation method. These power estimates are very  
386 similar to previous published estimates for Frequentist models (Dingemans & Dochter-  
387 mann, 2013). These methods also displayed the expected false positive rates (5%) under  
388 all simulated conditions (black points in Figure 6). The reduced method for estimating  
389 power, using the same null distribution for all simulation datasets within a particular  
390 data structure, generally gave a similar power to the other methods (Figure S9).

391 As with the p-values, power was not particularly sensitive to the measure of central  
392 tendency used, the highest power being seen in the mode with higher smoothing and the  
393 lowest power with the mode with less smoothing (Figure S9).

## 394 **Worked example - Random slopes**

395 As is often the case, the examples presented above are simplistic and empiricists com-  
396 monly encounter more complex questions and data structures in their studies. Here we  
397 outline a more realistically complex example where the permutation of datasets require  
398 some careful decisions.

399 Random slope models (where group-specific intercepts and slopes are modelled, also  
400 known as random regression) provide a good example of this complexity. We will fo-  
401 cus here on generating a null distribution for the estimate of among-group variance in  
402 slopes. This estimate is based upon the relationship between the predictor variable and  
403 response, the distribution of the response variable across groups, and the distribution of  
404 the predictor variable within and across groups. This provides us with four possibilities  
405 for permutation: 1) permuting the response variable (retains data structure and breaks  
406 all relationships with response); 2) permuting the predictor (retains the group data struc-  
407 ture, breaks link between predictor and response, and the distribution of the predictor  
408 across groups); 3) permuting the group identities (breaks the group data structure, but re-  
409 tains link between predictor and response); and 4) permuting the predictor within groups  
410 (retains the group data structure and the distribution of the predictor across groups, but  
411 breaks link between predictor and response). Additionally, we can also generate a null  
412 distribution through simulation, where we can simply simulate no among-group variance  
413 in slopes, adding the variance generated by the random slopes to the residual to ensure  
414 the same total phenotypic variance. Below we explore these different null distributions  
415 using a simulated and a real data set. Null distributions were generated based upon the  
416 analyzes of 100 null datasets.

## 417 **Simulated dataset**

418 We imagined a hypothetical researcher measuring the body mass of a bird species at  
419 different times of the day with the aim of studying how temperature affects body mass.  
420 The question of interest was to assess whether there is variation among individuals in  
421 how temperature affects their body mass. The (simulated) observed data set consisted of  
422 300 individuals measured 4 times each. Body mass and temperature were both normally  
423 distributed. Temperature was scaled to have a mean of 0 and variance of 1, and has an  
424 effect on body mass of 0.2 for the average individual. The simulated among individual  
425 variance in the intercepts was 0.2 and the phenotypic variance generated by variation  
426 in slopes was 0.1 (with no correlation among random slopes and intercepts), while the  
427 residual variance was set to 0.7 to ensure a total phenotypic variance not explained by  
428 the average effect of the environment was 1. Formulas to estimate the total phenotypic  
429 variance in random slope models can be found in [Allegue \*et al.\* \(2017\)](#) There were no  
430 systematic differences in the average temperature experienced by the different individuals.

## 431 **Real world dataset**

432 For our example with real data, we used a study on variation in the plastic aggressive  
433 response to intruders of great tits (*Parus major*) in a nestbox population in southern  
434 Germany ([Araya-Ajoy & Dingemanse, 2017](#)). Aggressiveness data were collected over a  
435 6-year period (2010–2015) for all male birds during their first breeding attempt each year.  
436 The aggression test started when a taxidermic mount of a male great tit was presented on  
437 a 1.2 m wooden pole with a playback song 1 m away from the subject's nest box. They  
438 subsequently recorded the behaviour of the focal male for a period of 3 min after it had  
439 entered a 15 m radius around the box. Simulated territorial intrusions were performed  
440 twice during the egg-laying stage and twice during the egg-incubation stage of each focal  
441 nest. Therefore, males had repeated measures both within- and among-years.

442 We analysed 2854 aggression tests performed to 1042 breeding attempts of 679 in-  
443 dividuals. The average number of years for which we obtained an individual’s reaction  
444 norm was 1.4, with 513, 142, 44, 8, 8 and 1 individual(s) sampled for one, two, three, four,  
445 five or six breeding attempt(s) (years), respectively. On average, we acquired 2.8 (out of  
446 4) data points for male aggressiveness per breeding attempt (i.e. year), because males  
447 did not always respond to the territorial intrusion experiment ([Araya-Ajoy & Dingem-  
448 manse, 2017](#)). Details of the experimental setup, and assayed behaviours, are provided in  
449 [Araya-Ajoy & Dingemanse \(2014\)](#). For the purpose of this paper, we used the subject’s  
450 minimum distance to the mount as a measure of aggressiveness because previous work  
451 implies that this behaviour represents a reliable predictor of the intensity of an aggressive  
452 response in both stages of breeding ([Araya-Ajoy & Dingemanse, 2014](#)).

## 453 **Random slope methods**

454 Both datasets were analysed using random slope mixed-effects models, specifying the en-  
455 vironmental predictor (temperature for the simulated example and breeding stage for the  
456 real example) as a fixed covariate, and random intercepts and environment slopes across  
457 individuals. We then generated 5 null distributions (4 permutations and 1 simulation),  
458 as outlined above, with which we compared the estimate of among individual variance in  
459 slopes from the observed data. Breeding stage (egg-laying versus egg-incubation) was first  
460 coded as zero (for laying) versus one (for incubation), and subsequently mean centred and  
461 standardized to standard deviation units. Models were fitted in a Bayesian framework,  
462 using Stan with the rstan package (version 2.21.3 [Stan Development Team, 2022a](#)). We  
463 specified weakly informative priors on the among-group and residual standard deviation.  
464 We ran three chains for the model of the simulated and real observed data with 5,500  
465 iterations and a warm-up period of 500 iterations. To decrease computational burden,  
466 the models for the permuted/simulated data sets were run for only one chain. We then  
467 generated five null distributions of posterior medians for each dataset, using the methods

468 described above.

## 469 **Random slope results**

470 The different types of null distributions provided the same qualitative results, support-  
471 ing the conclusion regarding among-individual variation in slopes, in both the real and  
472 simulated datasets (Fig 7). For these datasets, permuting individual identity created  
473 null distributions with a larger mean value of random slope variance (see Discussion for  
474 an explanation). It is important to note that these results relate only to this specific  
475 example and may not generalize to other studies. We therefore recommend exploring the  
476 particular consequences of using different types of permutations for specific datasets, if a  
477 reader wishes to use a permutation method.

## 478 **Discussion**

479 Through the use of simulations, we demonstrate the difficulties of summarising the poste-  
480 rior distributions of variance estimates from MCMC-based models. We describe different  
481 methods for generating null distributions that provide useful complimentary informa-  
482 tion alongside the presentation of central tendency and uncertainty that are generally  
483 reported. We also show a way in which null distributions could be used to derive a p-  
484 value, which is an easy addition to the statistics presented when summarizing a posterior  
485 distribution and also facilitates power analysis.

## 486 **Summary statistics**

487 Our experience in ecology and evolution is that both posterior mean and mode are com-  
488 monly, but inconsistently, presented without justification. For fixed effect parameter  
489 estimates, this is typically inconsequential, as the posteriors are usually symmetrically

490 distributed. When estimating variance components, however, our simulations show that  
491 depending upon the underlying parameter value, both of these measures can show large  
492 biases in opposite directions. When posterior distributions are close to zero and there  
493 *is* among-group variance, the posterior mode is very biased towards zero, whereas the  
494 posterior median and mean perform much better. On the other hand, if there is no  
495 among-group variance, the mode is by far the least biased. The mode, however, suffers  
496 further from subjectivity in its estimation. Our simulations also show that the estimation  
497 of the mode depends on the underlying algorithm for mode estimation. Unfortunately,  
498 the method of mode estimation is rarely justified or even stated in empirical papers. The  
499 mode also requires larger posterior distributions to be reliably estimated and will show  
500 greater variation between models/chains (Kruschke, 2015). Given this hidden ambiguity  
501 in the estimation of the mode, we would therefore cautiously recommend the presentation  
502 of the posterior median, or both median and mean, as a measure of central tenancy for  
503 variance components. This recommendation is based upon the median being generally  
504 less biased than the mean when power is low. Presenting both allows the discrepancy to  
505 be seen, showing that the distribution is near to zero and not symmetric, further stressing  
506 the uncertainty in these measures.

507 Upward biases in variance components have been seen before when power is low, but  
508 the dependence on the choice of the central tendency metric has not been highlighted.  
509 For example, Fay *et al.* (2022) note overestimation of variance components in Bernoulli  
510 models, with this overestimation decreasing in size as sample size and effect size increase.  
511 Fay *et al.* (2022) use the posterior mean as a summary statistic, and (as we show in  
512 Supplementary Figure S10) this bias will decrease (although not disappear completely)  
513 through the use of a posterior median. This is not just a bias in Bernoulli models, or in  
514 fact MCMC models (Figure S1), but a general property of variance components estimated  
515 with low power.

516 It is often argued that rather than presenting summary statistics, we should present

517 and interpret the whole posterior distribution, which are frequently presented using den-  
518 sity plots. Again, the underlying parameters of the kernel density estimation are usually  
519 not presented alongside the density plots, meaning the amount of smoothing is not doc-  
520 umented. A large degree of smoothing can hide asymmetry and/or bi-modality, and so  
521 change inferences. We therefore suggest the use of histograms over density plots in the  
522 presentation of posterior distributions, because although they are subject to the same  
523 smoothing problems, the degree of smoothing is explicit in the histogram, but hidden in  
524 the density plot. Alternatively, other plots that explicitly show the raw posterior samples  
525 (e.g. beeswarm plots) could be used (e.g. Figures 4 and 5).

## 526 **Null distributions**

527 The null distribution approaches outlined here are relatively easy to use, and allow quan-  
528 tification of confidence that a variance estimate is the result of a biological process rather  
529 than a consequence of the choice of priors and data structure. Importantly, the p-values  
530 based upon null distributions are not dependent upon what measure of central tendency  
531 is used. Such inferential statistics comparing the observed estimates with the null distri-  
532 butions can provide quantitative measures that can be reported alongside the observed  
533 estimates and uncertainty, and provides a useful tool for assessing the probability that  
534 variance components are non-zero and thereby supplement visual inspections of posterior  
535 distributions, or comparison of posterior mode, median and mean. Furthermore, they  
536 can serve as an objective and easy-to-communicate assessment of the biological relevance  
537 of an estimated variance component to the general public and policy makers, or for the  
538 statistical support of non-zero values for derived statistics like heritability, repeatability  
539 or evolvability. Common criticisms of p-values include that they are often misinterpreted  
540 or used for NHST. We would therefore recommend readers thinking of using the null  
541 distribution approach to acquaint themselves with the literature on these topics (some  
542 useful examples include [Wasserstein & Lazar, 2016](#); [Amrhein \*et al.\*, 2017](#); [McShane \*et al.\*,](#)

543 [2019; Amrhein \*et al.\*, 2019](#)). Importantly, p-values cannot demonstrate absence of effect,  
544 just confidence in difference from the null hypothesis (here no among-group variance).  
545 We believe generating null distributions will help empiricists understand these concepts,  
546 as they can be used to give a visual representation of what a p-value signifies.

547 As we illustrate in our examples of random slopes, there are different ways of per-  
548 muting datasets, which become more varied as the complexity of the data structure and  
549 model increase. Our example on random slope analysis demonstrated that these differ-  
550 ences can lead to qualitatively similar results, although whether they always or usually  
551 do so would require a much broader set of simulations than we report here. Interestingly,  
552 permuting individual identity created null distributions with noticeably larger values of  
553 random slope variance. We believe this is due to the existence of random slopes in the  
554 simulated and real data set generating heterogeneous residuals (i.e. variance in response  
555 changed with the environmental predictor) that were confounded with random slope vari-  
556 ation in the analyses of the null data sets (similar effects are also shown in [Ramakers  
557 \*et al.\*, 2020](#)). The other permutation methods break up the relationship between the  
558 predictor and response, and so the average estimate for the null distributions was lower.  
559 This illustrates how comparing the results of the different methods of null distributions  
560 generation may provide insights that may be used to inform the statistical inferences  
561 from estimated variance components.

562 In some instances, generating a null distribution using permutations may not be  
563 possible. For example, in event-history models of survival (where individuals have an  
564 entry for each time point where they are observed, in a sequence of 0's for time points  
565 they survive and a 1 for the time point after which they die). In this case, permuting the  
566 individual identifiers would fundamentally alter the data structure, meaning that some  
567 individuals had multiple deaths. This could be made to work in the context of an animal  
568 model, where the observed 0's and 1's could be interchanged between individuals, so that  
569 the same between individual structure was maintained, but the link with the pedigree

570 was broken. This serves to demonstrate that some care needs to be taken when assessing  
571 the suitability of permutations and how they impact the data structure on a case-by-  
572 case basis. Overall, we are not advocating a specific recipe for permutations here - it is  
573 likely context and question dependent. We instead advocate a simulation approach at  
574 the planning stage, using simulations to check in advance that the permutation design  
575 gives desired properties with your likely data structure.

576       Generating null distributions through simulation avoids many of the issues with the  
577 permutation approach, although it does not account so well for the particularities of each  
578 data set. Simulation has the advantage that it allows the structure of the data to be  
579 fully retained, a more fine-scale alternation of the variances in question, and it makes  
580 no additional assumptions than those already being made by the statistical model itself.  
581 Reassuringly, in our random slope example, the null distributions generated using the  
582 simulation method were similar to the other methods. We therefore cautiously recom-  
583 mend the use of this simulation method, as it is the most flexible for complex models.

584       These null distribution approaches are, however, computationally intensive and ap-  
585 plying them can take a long time depending upon the model complexity, the amount  
586 of data and the available computational resources. MCMC methods are often used for  
587 highly complex problems (e.g. double hierarchical GLMs; [Cleasby et al., 2015](#)), where  
588 running a large number of permutations may not be an option. The number of permuta-  
589 tions/simulations that are run affects the precision with which a p-value can be calculated  
590 and the minimum p-value that can be calculated - a null distribution of 100 can have a  
591 minimum p-value of 0.01 and vary by intervals of 0.01. This is why we would recommend  
592 a higher number of samples in the null distributions than we used here. However, we  
593 were able to produce meaningful results with 100 simulations, and even a few permuta-  
594 tions/simulations would give some idea (although much less reliably) of how incompatible  
595 the observed variance was with the range expected under the null hypothesis.

## 596 **Alternative approaches**

597 A p-value is defined as the probability that an estimate equal to or more extreme than  
598 the observed estimate would occur under the null hypothesis (i.e. if the true among-  
599 group variance is zero). It relies upon the distribution of p-values being uniform when  
600 the null hypothesis is true, a property that is expected to be invariant to sample size (as  
601 we show in Figure 4). P-values therefore provide support for the alternative hypothesis,  
602 but they do not provide support for the null hypothesis. The ROPE value and Bayes  
603 factors aim to assess actual support for the null hypothesis, and therefore depend upon  
604 sample size. Below we outline the potential issues that empiricists may encounter when  
605 trying to employ these methods.

606 The ROPE introduces another source of subjectivity into the analysis, because it  
607 involves an arbitrary threshold that needs to be defined. This is not trivial in the case  
608 of variance components, as small variances can have large knock-on effects. For example,  
609 [McFarlane \*et al.\* \(2015\)](#) find that maternal genetic effects account for 2% of variation  
610 in fitness, but this small amount predicts a 56% increase in mean lifetime reproductive  
611 success in less than 10 generations, which is highly biologically meaningful. [Bonnet \*et al.\*](#)  
612 [\(2022\)](#) address this by using simulations to demonstrate the biological relevance of the  
613 thresholds they use (0.01 and 0.001, for the variances not ICC). There is also discussion  
614 about whether the overlap of the whole posterior or the 95% credible interval should  
615 be used with ROPE ([Makowski \*et al.\*, 2019a](#); [Schwaferts & Augustin, 2020](#)). As with  
616 NHST, 95% is also an arbitrary cutoff, and so the ROPE would represent the overlap  
617 of two arbitrary thresholds. ROPE is often discussed in a context where a cost-benefit  
618 analysis can be used to work out the minimum effect size that warrants the use of a  
619 particular intervention, for example of medical interventions ([Kruschke, 2018](#)). Typically  
620 this is not relevant for research in ecology and evolution as, in many cases, it is of interest  
621 whether variance in a particular component exists, and if so its magnitude. We think  
622 there is clear application for using ROPE in fields like conservation, where interaction

623 with stakeholders requires thresholds over which decisions need to be made, but for many  
624 empiricists, ROPE requires more subjective decisions to be made and justified.

625 Bayes factors can be used to test the 'significance' of parameters in Bayesian mixed-  
626 effect models. However, the calculation of Bayes factors that allow inferences to be  
627 made about variance components is not straightforward. They require large posterior  
628 distributions for stable estimation and are sensitive to both prior and model specification  
629 (Gelman *et al.*, 2013; Navarro, 2019; Schad *et al.*, 2022) and there is some ambiguity in  
630 which models should be compared and what questions they answer (van Doorn *et al.*,  
631 2021). Bayes factors are also not implementable in all programs, including commonly  
632 used programs in ecology and evolution (e.g. MCMCglmm). Our approach provides  
633 an alternative to this method, which is easily implemented and allows straightforward  
634 interpretation with reference to the probability that the estimate obtained is inconsistent  
635 with the data structure and model specification alone.

## 636 **Power analysis and possible alternatives**

637 Power analysis is controversial as it relies on NHST. NHST is controversial because its  
638 misuse has been attributed to scientific misconduct and the replication crisis (Wasserstein  
639 & Lazar, 2016; Amrhein *et al.*, 2017; McShane *et al.*, 2019; Amrhein *et al.*, 2019), issues  
640 which relate to the use of p-values *after* data collection and analysis. Power analysis, how-  
641 ever, serves a clear purpose in aiding experimental design, and is conducted *pre*-analysis,  
642 and so is perhaps not subject to the same criticisms. Suggested alternatives, such as Type  
643 M and Type S error, also rely upon calculation of p-values and definition of an arbitrary  
644 alpha value, and are both a simple function of power (Gelman & Carlin, 2014). Type S  
645 error (proportion of significant estimates that have the opposite sign) is not relevant for  
646 variance components. Type M (absolute relative bias of significant estimates) gives some  
647 additional information but, unlike power, it is affected by the measure of central tendency  
648 that is chosen (Figure S11). Power can also be seen as a description of the distribution

649 of p-values expected for a given effect size and data structure. Other descriptions of this  
650 distribution (e.g. the mean) would be simple functions of the power, but the common  
651 use of this metric makes it more widely understood. An alternative to power would be to  
652 design studies around a desired level of precision in estimates. Although this works for  
653 unbounded parameters, precision is difficult to interpret for variance components, and  
654 SE will decrease as true value gets closer to zero, not because precision increases, but  
655 because it is limited by zero (see Figure S4). We would therefore suggest that power still  
656 provides a suitable metric for designing studies to estimate variance components.

657 We show two methods of power analysis based upon null distributions. The first (full)  
658 involves generating p-values for each simulated dataset by generating a null distribution  
659 for that dataset. This method is highly computationally intensive as it involves running  
660 a certain number of simulations multiplied by the number of permutations/simulations  
661 models, which could realistically be one million models per parameter. Our alternative  
662 method (reduced) is to generate a single null distribution for each data structure, and  
663 generate p-values by comparing the parameter estimates from the simulated datasets to  
664 this single null distribution. This method gives similar results to the full approach and  
665 is massively less computationally intensive (requiring running 2000 models rather than  
666 a million for each set of parameters). The disadvantage is that the false positive rate  
667 cannot be calculated.

668 Even if power is not the intended use (or there is an objection to arbitrary alpha  
669 values), these simulations can serve an extremely useful purpose before studies are con-  
670 ducted. First, these simulations allow an empiricist to consider the distribution of p-values  
671 expected under a given effect size and design (note that power is essentially a description  
672 of the shape of this distribution). Second, the null distribution of point estimates can  
673 be considered - this enables the distribution of effect sizes that can occur under the null  
674 hypothesis to be visualised. Even if an empiricist does not want to calculate a p-value,  
675 creating a null distribution is still a powerful way of seeing the distribution of estimates

676 that would be generated with no among-group variance, and would serve to encourage  
677 caution in how results that lie within that distribution are interpreted.

## 678 **Recommendations**

- 679 1. Using the posterior median as a measure of central tendency for posterior distri-  
680 butions of variance components from MCMC-based models. Our results show that  
681 the median is the least biased estimate, but will overestimate variances when power  
682 is low. Reporting multiple measures of central tendency allows any asymmetry in  
683 the posterior to be made obvious.
- 684 2. Reporting of smoothing values in kernel estimation. Kernel density estimation is  
685 commonly used for estimating the posterior mode and creating density plots. The  
686 parameters used in this estimation are seldom reported, but can have a large impact  
687 on interpretation. We advise the reporting of parameters in the kernel density  
688 estimation, or the use of more explicit methods of plotting posterior distributions,  
689 such as histograms.
- 690 3. Using null distributions for inference. Null distributions provide a way of putting the  
691 observed parameter estimates into a context expected under an explicitly defined  
692 null hypothesis (i.e. no among-group variance). Null distributions can be created in  
693 multiple ways, but they are most easily controlled when generated using simulations.  
694 As with many aspects of statistical analysis, there are many decisions relating to  
695 generating null distributions that may have an affect on the results. Therefore,  
696 these methods should be defined pre-analysis, in order to reduce researcher degrees  
697 of freedom.
- 698 4. Using a null distribution to estimate power. As well as aiding *post-hoc* inference,  
699 null distributions can be used for power analysis. We provide details of a method  
700 for doing so that does not present a large computational burden.

## 701 **Acknowledgments**

702 We would like to thank the other members of the Statistical Quantification of Individual  
703 Differences (SQuID) working group, and the Wild Evolution and Statistics in Ecology  
704 and Evolution Discussion groups at the University of Edinburgh for valuable feedback on  
705 the ideas presented here. SQuID workshops in 2022 and JLP were funded by a Research  
706 Council of Norway INTPART project number 309356 grant to JW. YGA was supported  
707 by the Research Council of Norway project number 325826. HS were supported by  
708 the German Research Foundation (DFG, 215/543-1, 316099922). DFW was supported  
709 by the U.S. National Science Foundation. HA was supported by the Natural Sciences  
710 and Engineering Research Council of Canada (CGSD3-504399-2017) and the Fond de  
711 Recherche du Québec - Nature et Technologies (FRQNT; 283511).

## 712 **Conflict of Interest statement**

713 The authors declare no conflict of interest.

## 714 **Author Contributions**

715 JLP, CK, NJD, DFW and YGAA conceived the ideas; JLP, YGAA, HS and NAD de-  
716 signed methodology; JLP and YGAA ran the simulations; All authors contributed to  
717 the interpretation of results; JLP and YGAA led the writing of the manuscript, and all  
718 authors contributed critically to the drafts and gave final approval for publication.

## 719 **Data and code availability**

720 All code and generated data for the simulated examples are deposited in [https://](https://github.com/squidgroup/null_distributions)  
721 [github.com/squidgroup/null\\_distributions](https://github.com/squidgroup/null_distributions)

## 722 References

- 723 Allegue, H., Araya-Ajoy, Y.G., Dingemanse, N.J., Dochtermann, N.A., Garamszegi, L.Z.,  
724 Nakagawa, S., Réale, D., Schielzeth, H. & Westneat, D.F. (2017) Statistical Quantifi-  
725 cation of Individual Differences (SQuID): an educational and statistical tool for under-  
726 standing multilevel phenotypic data in linear mixed models. *Methods in Ecology and*  
727 *Evolution*, **8**, 257–267. eprint: [https://onlinelibrary.wiley.com/doi/pdf/10.1111/2041-](https://onlinelibrary.wiley.com/doi/pdf/10.1111/2041-210X.12659)  
728 [210X.12659](https://onlinelibrary.wiley.com/doi/pdf/10.1111/2041-210X.12659), <https://dx.doi.org/10.1111/2041-210X.12659>.
- 729 Amrhein, V., Greenland, S. & McShane, B. (2019) Scientists rise up against statistical  
730 significance. *Nature*, **567**, 305–307. <https://dx.doi.org/10.1038/d41586-019-00857-9>.
- 731 Amrhein, V., Korner-Nievergelt, F. & Roth, T. (2017) The earth is flat ( $p > 0.05$ ):  
732 Significance thresholds and the crisis of unreplicable research. *PeerJ*, **5**, e3544.  
733 <https://dx.doi.org/10.7717/peerj.3544>.
- 734 Araya-Ajoy, Y.G. & Dingemanse, N.J. (2014) Characterizing behavioural 'characters':  
735 an evolutionary framework. *Proceedings of the Royal Society of London Series B*, **281**,  
736 20132645. <https://dx.doi.org/10.1098/rspb.2013.2645>.
- 737 Araya-Ajoy, Y.G. & Dingemanse, N.J. (2017) Repeatability, heritability, and age-  
738 dependence of seasonal plasticity in aggressiveness in a wild passerine bird. *Journal of*  
739 *Animal Ecology*, **86**, 227–238. <https://dx.doi.org/10.1111/1365-2656.12621>.
- 740 Bates, D., Mächler, M., Bolker, B. & Walker, S. (2015) Fitting linear  
741 mixed-effects models using lme4. *Journal of Statistical Software*, **67**, 1–48.  
742 <https://dx.doi.org/10.18637/jss.v067.i01>.
- 743 Bell, A.M., Hankison, S.J. & Laskowski, K.L. (2009) The repeatability of behaviour: a  
744 meta-analysis. *Animal Behaviour*, **77**, 771–783. Publisher: Elsevier Ltd ISBN: 0003-  
745 3472, <https://dx.doi.org/10.1016/j.anbehav.2008.12.022>.

746 Bolker, B.M., Brooks, M.E., Clark, C.J., Geange, S.W., Poulsen, J.R., Stevens,  
747 M.H.H. & White, J.S.S. (2009) Generalized linear mixed models: A practical  
748 guide for ecology and evolution. *Trends in Ecology and Evolution*, **24**, 127–135.  
749 <https://dx.doi.org/10.1016/j.tree.2008.10.008>.

750 Bonnet, T., Morrissey, M.B., de Villemereuil, P., Alberts, S.C., Arcese, P., Bailey, L.D.,  
751 Boutin, S., Brekke, P., Brent, L.J.N., Camenisch, G., Charmantier, A., Clutton-Brock,  
752 T.H., Cockburn, A., Coltman, D.W., Courtiol, A., Davidian, E., Evans, S.R., Ewen,  
753 J.G., Festa-Bianchet, M., de Franceschi, C., Gustafsson, L., Höner, O.P., Houslay,  
754 T.M., Keller, L.F., Manser, M., McAdam, A.G., McLean, E., Nietlisbach, P., Osmond,  
755 H.L., Pemberton, J.M., Postma, E., Reid, J.M., Rutschmann, A., Santure, A.W.,  
756 Sheldon, B.C., Slate, J., Teplitsky, C., Visser, M.E., Wachter, B. & Kruuk, L.E.B.  
757 (2022) Genetic variance in fitness indicates rapid contemporary adaptive evolution in  
758 wild animals. *Science*, **376**, 1012–1016. <https://dx.doi.org/10.1126/science.abk0853>.

759 Cleasby, I.R., Nakagawa, S. & Schielzeth, H. (2015) Quantifying the predictability  
760 of behaviour: Statistical approaches for the study of between-individual variation  
761 in the within-individual variance. *Methods in Ecology and Evolution*, **6**, 27–37.  
762 <https://dx.doi.org/10.1111/2041-210X.12281>.

763 de Villemereuil, P., Gimenez, O. & Doligez, B. (2013) Comparing parent–offspring re-  
764 gression with frequentist and Bayesian animal models to estimate heritability in wild  
765 populations: A simulation study for Gaussian and binary traits. *Methods in Ecology*  
766 *and Evolution*, **4**, 260–275. <https://dx.doi.org/10.1111/2041-210X.12011>.

767 Dingemanse, N.J. & Dochtermann, N.A. (2013) Quantifying individual variation in be-  
768 haviour: Mixed-effect modelling approaches. *Journal of Animal Ecology*, **82**, 39–54.  
769 <https://dx.doi.org/10.1111/1365-2656.12013>.

770 Fay, R., Authier, M., Hamel, S., Jenouvrier, S., van de Pol, M., Cam, E., Gaillard, J.M.,  
771 Yoccoz, N.G., Acker, P., Allen, A., Aubry, L.M., Bonenfant, C., Caswell, H., Coste,

772 C.F.D., Larue, B., Le Coeur, C., Gamelon, M., Macdonald, K.R., Moiron, M., Nicol-  
773 Harper, A., Pelletier, F., Rotella, J.J., Teplitsky, C., Touzot, L., Wells, C.P. & Sæther,  
774 B.E. (2022) Quantifying fixed individual heterogeneity in demographic parameters:  
775 Performance of correlated random effects for Bernoulli variables. *Methods in Ecology*  
776 *and Evolution*, **13**, 91–104. <https://dx.doi.org/10.1111/2041-210X.13728>.

777 Fitzmaurice, G.M., Lipsitz, S.R. & Ibrahim, J.G. (2007) A Note on Permutation Tests  
778 for Variance Components in Multilevel Generalized Linear Mixed Models. *Biometrics*,  
779 **63**, 942–946. <https://dx.doi.org/10.1111/j.1541-0420.2007.00775.x>.

780 Gelman, A., Carlin, J.B., Stern, H.S., Dunson, D.B., Vehtari, A. & Rubin, D.B. (2013)  
781 *Bayesian Data Analysis*. Chapman and Hall/CRC, 3rd edition.

782 Gelman, A., Hill, J. & Vehtari, A. (2020) *Regression and Other Stories*. Cambridge  
783 University Press, Cambridge.

784 Gelman, A. (2006) Prior distributions for variance parameters in hierarchical models.  
785 *Bayesian Analysis*, **1**, 515–533.

786 Gelman, A. & Carlin, J. (2014) Beyond Power Calculations: Assessing Type S (Sign)  
787 and Type M (Magnitude) Errors. *Perspectives on Psychological Science*, **9**, 641–651.  
788 <https://dx.doi.org/10.1177/1745691614551642>.

789 Gilks, W.R., Thomas, A. & Spiegelhalter, D.J. (1994) A Language and Program for  
790 Complex Bayesian Modelling. *Journal of the Royal Statistical Society Series D (The*  
791 *Statistician)*, **43**, 169–177. <https://dx.doi.org/10.2307/2348941>.

792 Hadfield, J.D. (2010) MCMC methods for multi-response generalized linear mixed mod-  
793 els: The {MCMCglmm} {R} package. *Journal of Statistical Software*, **33**, 1–22.  
794 <https://dx.doi.org/10.1002/ana.23792>.

795 Hadfield, J.D. & Nakagawa, S. (2010) General quantitative genetic methods for  
796 comparative biology: Phylogenies, taxonomies and multi-trait models for contin-

797 uous and categorical characters. *Journal of Evolutionary Biology*, **23**, 494–508.  
798 <https://dx.doi.org/10.1111/j.1420-9101.2009.01915.x>.

799 Harrison, X.A., Donaldson, L., Correa-Cano, M.E., Evans, J., Fisher, D.N., Good-  
800 win, C.E.D., Robinson, B.S., Hodgson, D.J. & Inger, R. (2018) A brief introduction  
801 to mixed effects modelling and multi-model inference in ecology. *PeerJ*, **6**, e4794.  
802 <https://dx.doi.org/10.7717/peerj.4794>.

803 Held, L. & Sabanés Bové, D. (2020) *Likelihood and Bayesian Inference*, volume 10.  
804 Springer.

805 Henderson, C.R. (1988) Theoretical basis and computational methods for a number of  
806 different animal models. *Journal of Dairy Science*, **71**, 1–16.

807 Houle, D. (1992) Comparing evolvability and variability of quantitative traits. *Genetics*,  
808 **130**, 195–204. <https://dx.doi.org/citeulike-article-id:10041224>.

809 Kay, M. (2022) *ggdist: Visualizations of Distributions and Uncertainty*. R package version  
810 3.2.0.

811 Kruschke, J. (2015) *Doing Bayesian Data Analysis*. Academic Press/Elsevier, second  
812 edition.

813 Kruschke, J. (2018) Rejecting or Accepting Parameter Values in Bayesian Estima-  
814 tion. *Advances in Methods and Practices in Psychological Science*, **1**, 270–280.  
815 <https://dx.doi.org/10.1177/2515245918771304>.

816 Kruuk, L.E.B. (2004) Estimating genetic parameters in natural populations using the  
817 “animal model”. *Philosophical Transactions of the Royal Society of London B*, **359**,  
818 873–890. <https://dx.doi.org/10.1098/rstb.2003.1437>.

819 Lakens, D., Scheel, A.M. & Isager, P.M. (2018) Equivalence Testing for Psychological  
820 Research: A Tutorial. *Advances in Methods and Practices in Psychological Science*, **1**,  
821 259–269. <https://dx.doi.org/10.1177/2515245918770963>.

- 822 Lehmann, E.L. & Romano, J.P. (2005) *Testing Statistical Hypotheses*. Springer Texts in  
823 Statistics. Springer, New York, 3rd ed edition.
- 824 Lemoine, N.P. (2019) Moving beyond noninformative priors: Why and how to  
825 choose weakly informative priors in Bayesian analyses. *Oikos*, **128**, 912–928.  
826 <https://dx.doi.org/10.1111/oik.05985>.
- 827 Makowski, D., Ben-Shachar, M.S., Chen, S.H.A. & Lüdecke, D. (2019a) Indices of Effect  
828 Existence and Significance in the Bayesian Framework. *Frontiers in Psychology*, **10**,  
829 2767. <https://dx.doi.org/10.3389/fpsyg.2019.02767>.
- 830 Makowski, D., Ben-Shachar, M.S. & Lüdecke, D. (2019b) bayestestr: Describing effects  
831 and their uncertainty, existence and significance within the bayesian framework. *Jour-*  
832 *nal of Open Source Software*, **4**, 1541. <https://dx.doi.org/10.21105/joss.01541>.
- 833 McElreath, R. (2020) *Statistical Rethinking: A Bayesian Course with Examples in R and*  
834 *Stan*. Chapman and Hall/CRC, 2nd edition.
- 835 McFarlane, S.E., Gorrell, J.C., Coltman, D.W., Humphries, M.M., Boutin, S. & Mcadam,  
836 A.G. (2015) The nature of nurture in a wild mammal’s fitness. *Proceedings of the Royal*  
837 *Society of London B*, **282**, 1–7.
- 838 McShane, B.B., Gal, D., Gelman, A., Robert, C. & Tackett, J.L. (2019)  
839 Abandon Statistical Significance. *The American Statistician*, **73**, 235–245.  
840 <https://dx.doi.org/10.1080/00031305.2018.1527253>.
- 841 Morey, R.D., Romeijn, J.W. & Rouder, J.N. (2016) The philosophy of bayes factors and  
842 the quantification of statistical evidence. *Journal of Mathematical Psychology*, **72**,  
843 6–18. <https://dx.doi.org/10.1016/j.jmp.2015.11.001>.
- 844 Nakagawa, S. & Schielzeth, H. (2010) Repeatability for Gaussian and non-Gaussian data:  
845 A practical guide for biologists. *Biological Reviews of the Cambridge Philosophical*  
846 *Society*, **85**, 935–56. <https://dx.doi.org/10.1111/j.1469-185X.2010.00141.x>.

- 847 Navarro, D.J. (2019) Between the Devil and the Deep Blue Sea: Tensions Between Sci-  
848 entific Judgement and Statistical Model Selection. *Computational Brain & Behavior*,  
849 **2**, 28–34. <https://dx.doi.org/10.1007/s42113-018-0019-z>.
- 850 O’Hara, R.B., Cano, J.M., Ovaskainen, O., Teplitsky, C. & Alho, J.S. (2008) Bayesian  
851 approaches in evolutionary quantitative genetics. *Journal of Evolutionary Biology*, **21**,  
852 949–957. <https://dx.doi.org/10.1111/j.1420-9101.2008.01529.x>.
- 853 O’Hara, R.B. & Merilä, J. (2005) Bias and precision in QST esti-  
854 mates: Problems and some solutions. *Genetics*, **171**, 1331–1339.  
855 <https://dx.doi.org/10.1534/genetics.105.044545>.
- 856 Pesarin, F. & Salmaso, L. (2010) *Permutation Tests for Complex Data*. John Wiley &  
857 Sons, Ltd, first edition.
- 858 Pick, J.L. (2022) *squidSim: a flexible simulation tool for linear mixed models*. R package  
859 version 0.1.0.
- 860 Plummer, M. (2003) Jags: A program for analysis of bayesian graphical models using  
861 gibbs sampling. *3rd International Workshop on Distributed Statistical Computing (DSC*  
862 *2003); Vienna, Austria*, **124**.
- 863 R Core Team (2022) *R: A Language and Environment for Statistical Computing*. R  
864 Foundation for Statistical Computing, Vienna, Austria.
- 865 Ramakers, J.J.C., Visser, M.E. & Gienapp, P. (2020) Quantifying individual variation  
866 in reaction norms: Mind the residual. *Journal of Evolutionary Biology*, **33**, 352–366.  
867 <https://dx.doi.org/10.1111/jeb.13571>.
- 868 Samuh, M.H., Grilli, L., Rampichini, C., Salmaso, L. & Lunardon, N. (2012)  
869 The Use of Permutation Tests for Variance Components in Linear Mixed Mod-  
870 els. *Communications in Statistics - Theory and Methods*, **41**, 3020–3029.  
871 <https://dx.doi.org/10.1080/03610926.2011.587933>.

- 872 Schad, D.J., Nicenboim, B., Bürkner, P.C., Betancourt, M. & Vasishth, S. (2022) Work-  
873 flow techniques for the robust use of bayes factors. *Psychological Methods*, pp. No  
874 Pagination Specified–No Pagination Specified. Place: US Publisher: American Psy-  
875 chological Association, <https://dx.doi.org/10.1037/met0000472>.
- 876 Schwaferts, P. & Augustin, T. (2020) Bayesian decisions using regions of practical equiv-  
877 alence (rope): Foundations.
- 878 Sheather, S.J. & Jones, M.C. (1991) A Reliable Data-Based Bandwidth Selection Method  
879 for Kernel Density Estimation. *Journal of the Royal Statistical Society Series B*  
880 (*Methodological*), **53**, 683–690.
- 881 Silverman, B.W. (1986) *Density Estimation for Statistics and Data Analysis*. Chapman  
882 and Hall, London.
- 883 Stan Development Team (2022a) RStan: the R interface to Stan. R package version  
884 2.21.3.
- 885 Stan Development Team (2022b) Stan modeling language users guide and reference man-  
886 ual. Version 2.3.
- 887 Stoffel, M.A., Nakagawa, S. & Schielzeth, H. (2017) rptR: Repeatability estimation and  
888 variance decomposition by generalized linear mixed-effects models. *Methods in Ecology*  
889 *and Evolution*, **8**, 1639–1644. <https://dx.doi.org/10.1111/2041-210X.12797>.
- 890 van Doorn, J., Aust, F., Haaf, J.M., Stefan, A.M. & Wagenmakers, E.J. (2021) Bayes Fac-  
891 tors for Mixed Models. *Computational Brain & Behavior*, pp. 1–13. Company: Springer  
892 Distributor: Springer Institution: Springer Label: Springer Publisher: Springer Inter-  
893 national Publishing, <https://dx.doi.org/10.1007/s42113-021-00113-2>.
- 894 Wasserstein, R.L. & Lazar, N.A. (2016) The ASA Statement on p-Values:  
895 Context, Process, and Purpose. *The American Statistician*, **70**, 129–133.  
896 <https://dx.doi.org/10.1080/00031305.2016.1154108>.

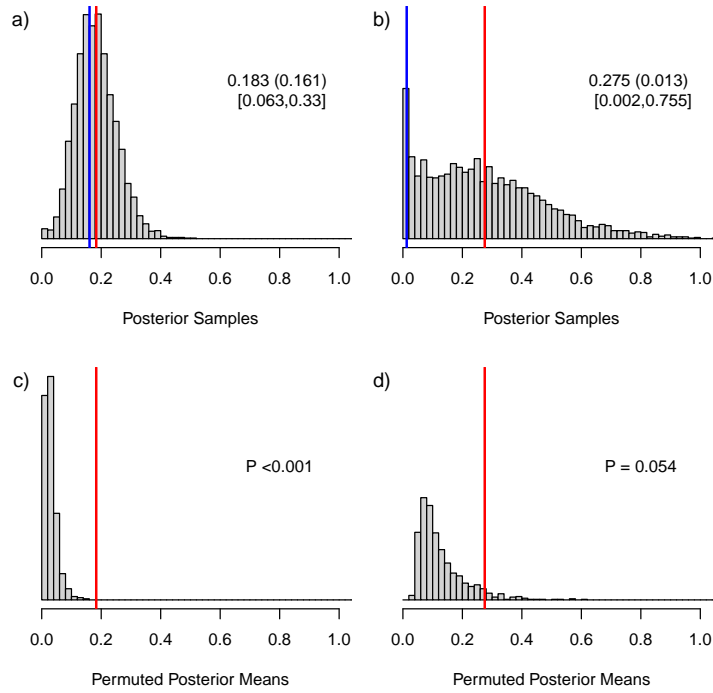


Figure 1: Posterior distributions of variance estimates for two different scenarios (a and b) and their respective null distributions (c and d) generated using permutations. Example a) shows a symmetric posterior distribution far away from zero with close agreement between the posterior mean (red lines) and mode (blue line), whilst b) shows an asymmetric posterior distribution close to zero, with clear divergence between the posterior mean and mode. c) and d) show null distributions of posterior means generated through permuting the datasets, and corresponding p-values, of a) and b), respectively. The values given in a) and b) correspond to mean (mode) [CRIs]. Both datasets were simulated with among-group variances of 0.2, but with differing sample sizes; a) with 80 groups and 4 observations per group; b) with 40 groups and 2 observations per group.

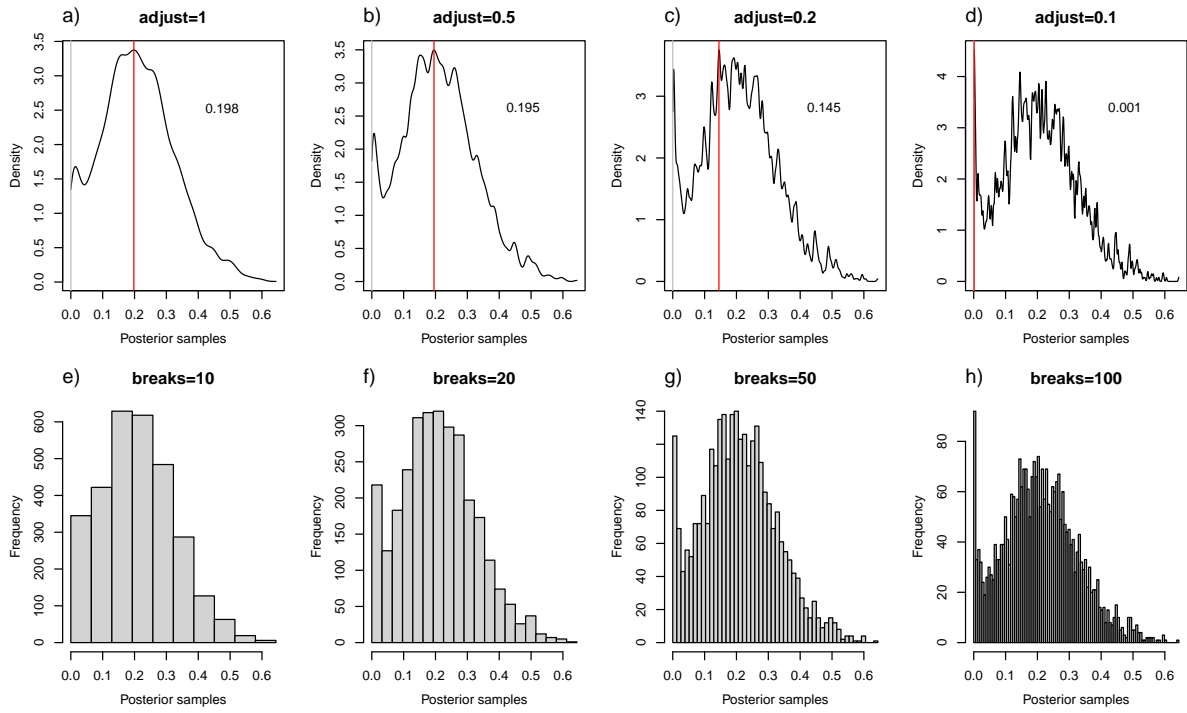


Figure 2: The effect of bandwidth choice on the estimation of the posterior mode. Top row shows kernel densities of the same posterior distribution, estimated with different bandwidth scalings, from 1 in a) to 0.1 in d). Red lines shows the posterior modes estimated from that scaling. Bottom row shows the equivalent histograms for comparison.

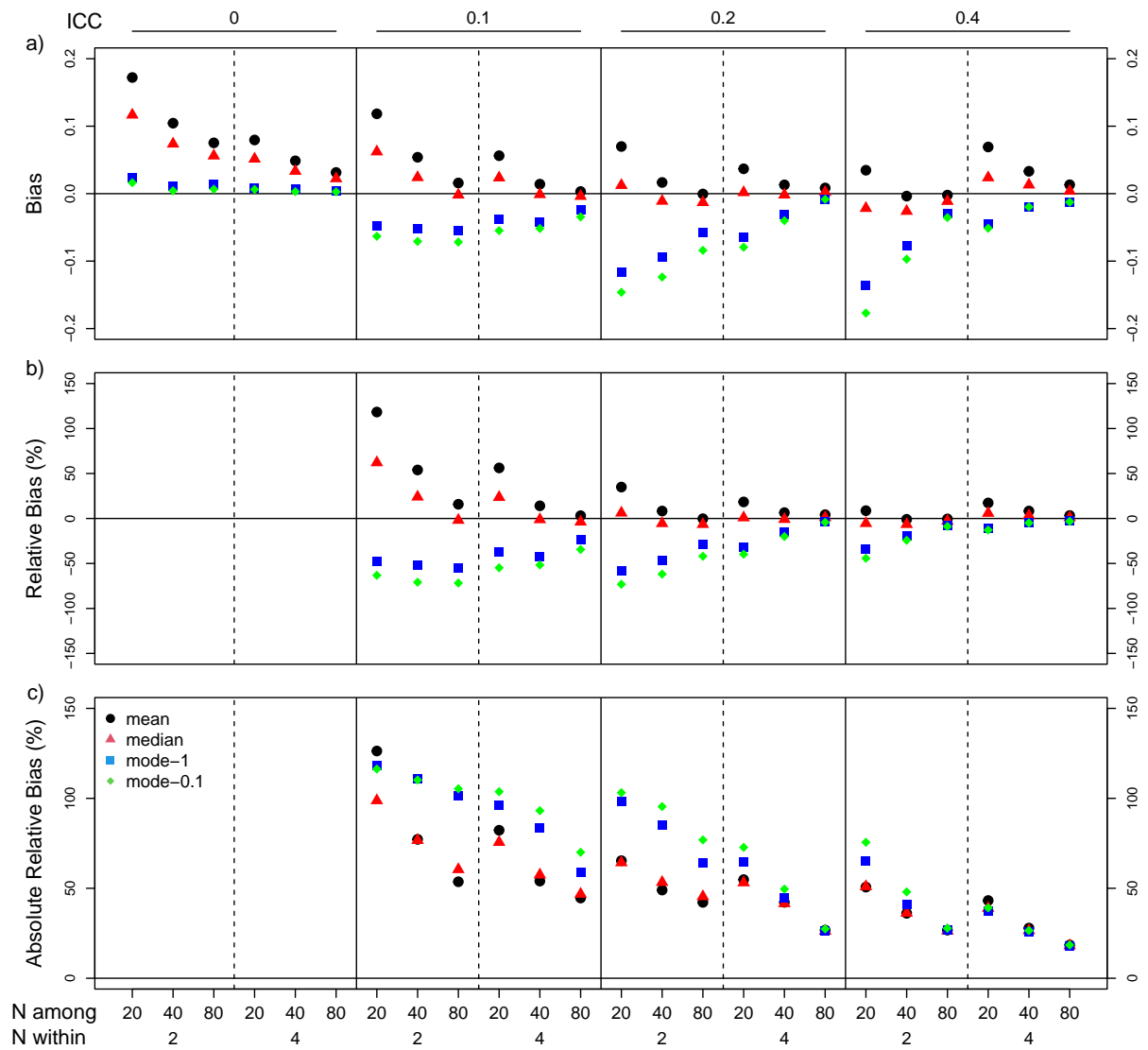


Figure 3: Bias (a), relative bias (b) and absolute relative bias (c) of posterior mean, median and mode of variance components from simulations varying in among group variance (ICC - 0, 0.1, 0.2, and 0.4) and sample size within (2 or 4) and among (20, 40, 80) groups. Two posterior modes were estimated: mode-1 and mode-0.1 with more and less smoothing, respectively (see text for more details).

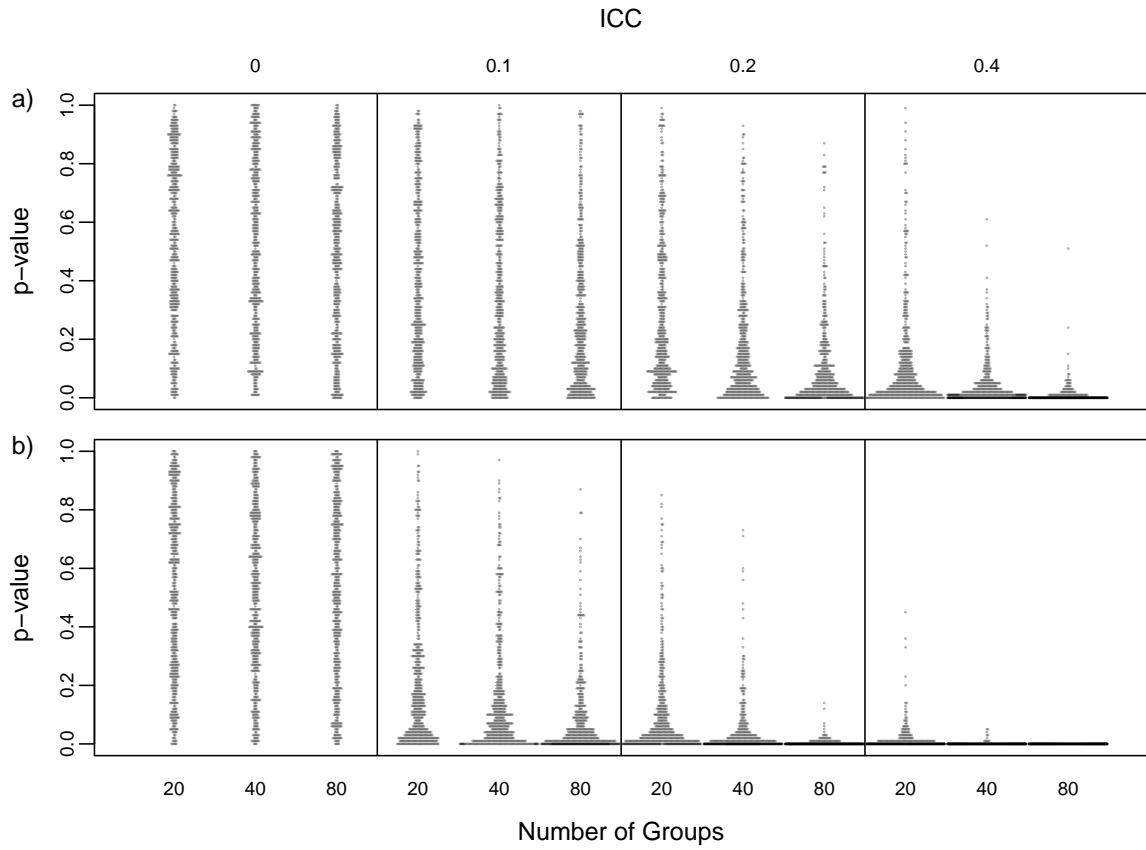


Figure 4: Distribution of  $p$ -values estimated using the posterior median and null distributions generated through simulations for datasets varying in among-group variance ( $ICC = 0, 0.1, 0.2, \text{ and } 0.4$ ) and sample size among (20, 40, 80) groups. Example a) shows a within group sample size of 2, and b) a within group sample size of 4.

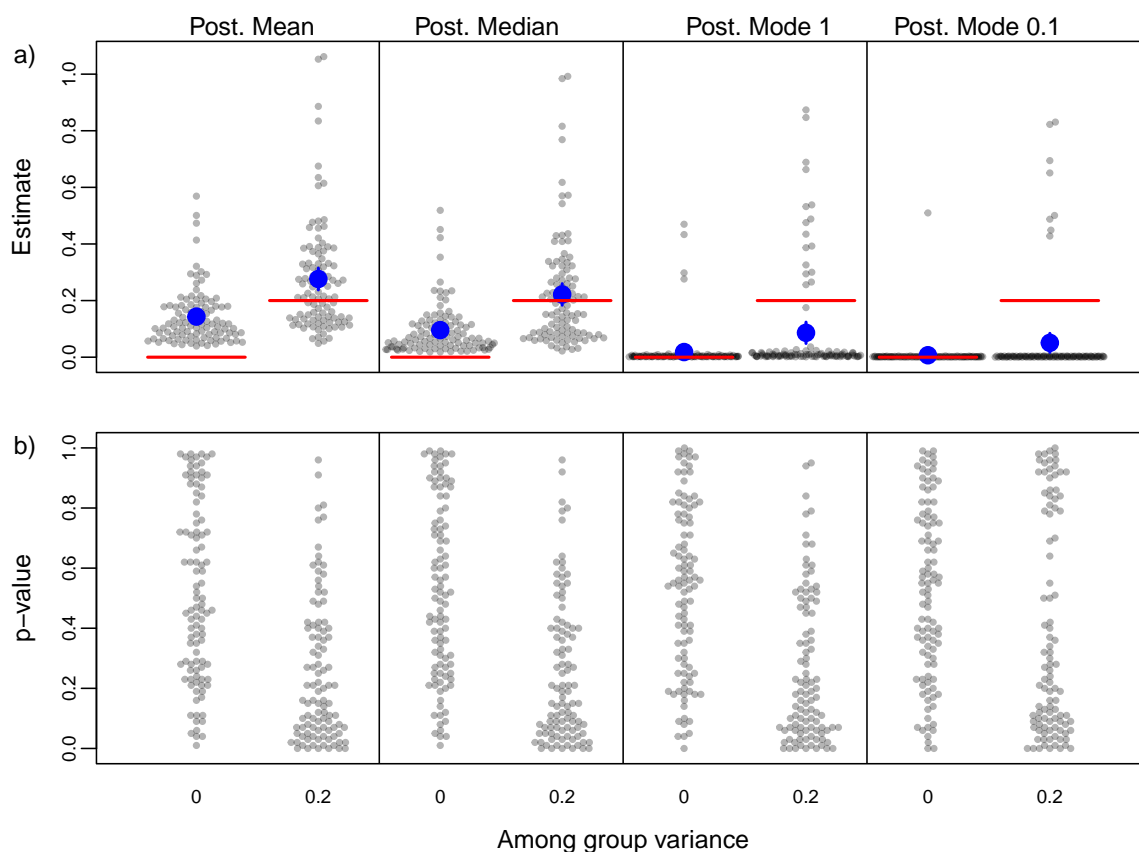


Figure 5: Sampling distributions of parameter estimates (a) and p-values (b) from GLMMs using different measures of central tendency. Two posterior modes were estimated: mode-1 and mode-0.1 with more and less smoothing, respectively (see text for more details). In a) red lines show simulated values, and blue points and error bars show mean and standard error of the sampling distributions. The p-values were generated using null distributions generated through simulation.

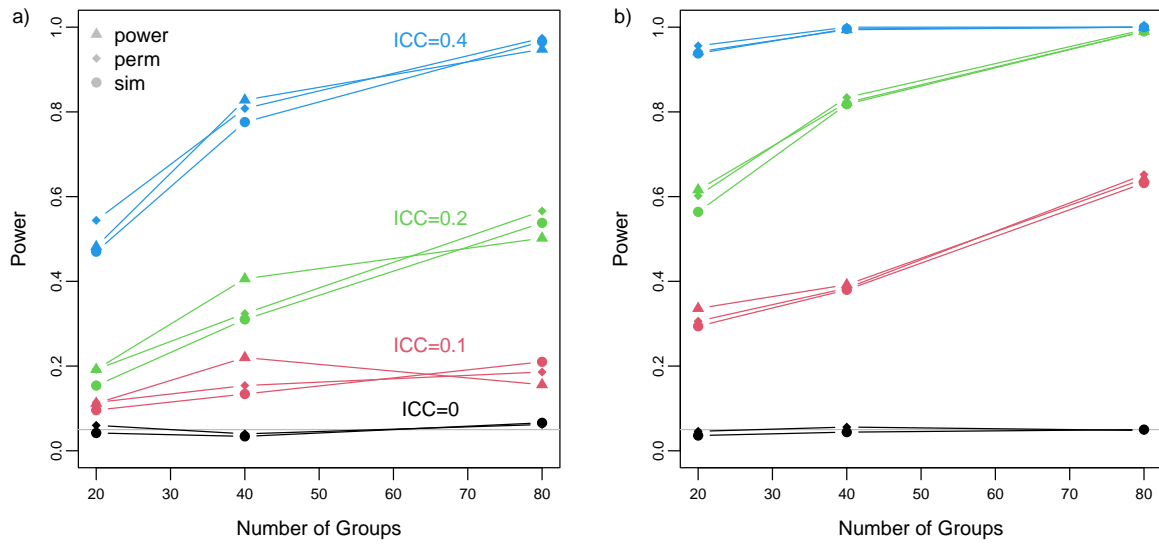


Figure 6: Comparisons of power calculated using permutation (*perm*), simulation (*sim*) or a global null distribution (*power*). For each within-group sample size of a) 2 and b) 4, we show results for four among-group variances (0, 0.1, 0.2 and 0.4) and three among-group sample sizes (20, 40 and 80). Power was calculated using posterior medians.

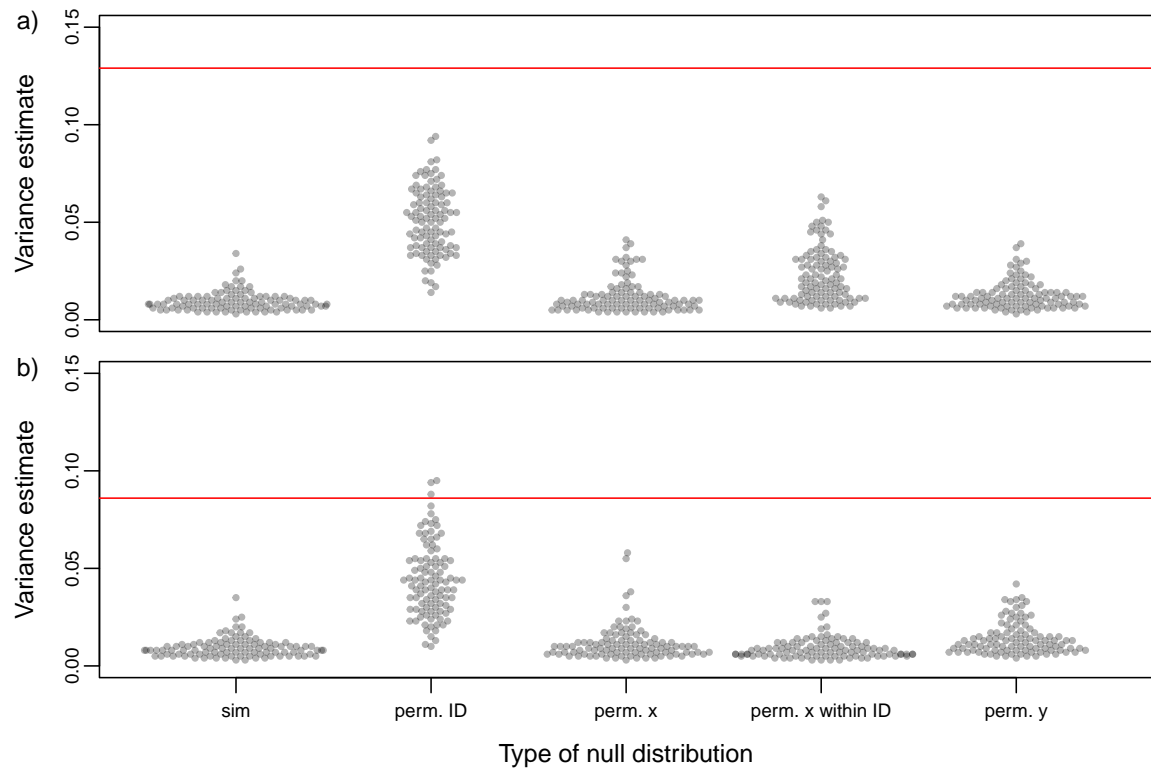


Figure 7: Null distributions of posterior medians generated with five different methods (see main text), from a) a simulated dataset, and b) a real dataset on aggressiveness in great tits. Red line represents posterior median estimated from original dataset.

## 898 **Supplementary Materials**

### 899 **Supplementary Methods**

#### 900 **Simulations based on [Fay et al. \(2022\)](#)**

901 We simulated datasets based on [Fay et al. \(2022\)](#), but ran simplified models (univariate  
902 instead of bivariate), as the purpose was simply to demonstrate the effect of different  
903 measures of central tendency on the bias in these models. We simulated data with the  
904 same parameters of one set of simulation in [Fay et al. \(2022\)](#) - fast life history and  
905 low heterogeneity. We simulated the probability of survival as 0.5 and probability of  
906 reproduction as 0.7, standard deviations on the latent scale of 0.2 for both survival and  
907 reproduction and a correlation of 0.6 between the two. We simulated 100 datasets from  
908 sample sizes of 250, 500, 1000, 2000, 4000 individuals. For each simulated dataset we ran  
909 a binomial GLMM, with random effects of individual identity using Stan with the rstan  
910 package (version 2.21.3 [Stan Development Team, 2022a](#)). We specified weakly informative  
911 priors on the among-group standard deviations (half-Cauchy distribution with scale 2),  
912 and ran one chain for each model with 7500 iterations and a warm-up period of 2000  
913 iterations. We then estimated the posterior mean, median and 2 modes as in the main  
914 text.

915 **Supplementary Figures**

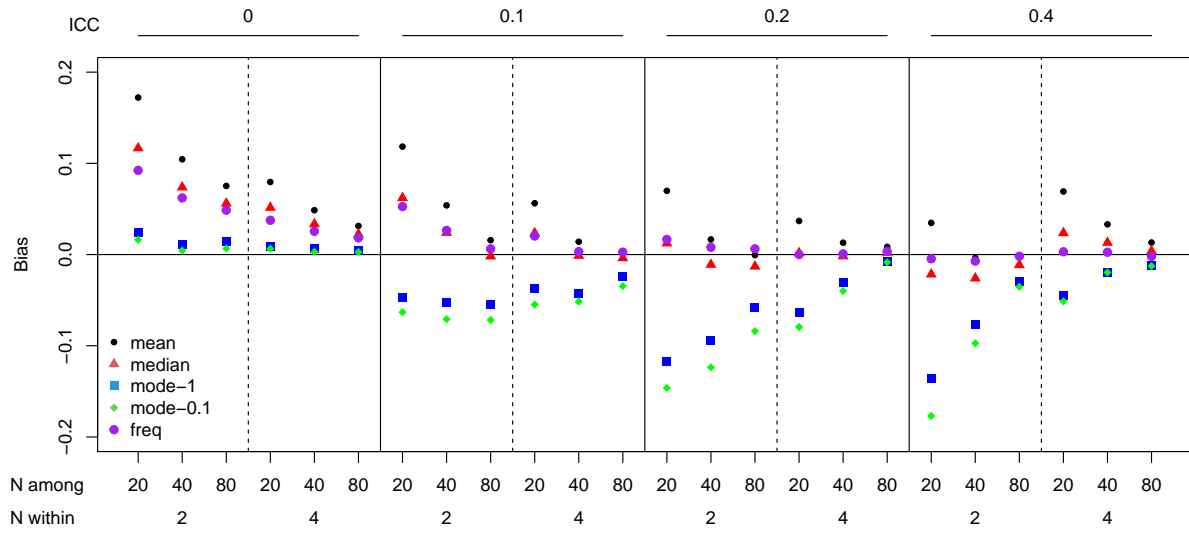


*Figure S1: Bias of Frequentist estimates alongside posterior mean, median and mode of variance components, from simulations varying in among-group variance (ICC - 0, 0.1, 0.2, and 0.4) and sample size within (2 or 4) and among (20, 40, 80) groups. Two posterior modes were estimated; mode-1 and mode-0.1 with more and less smoothing, respectively (see text for more details).*

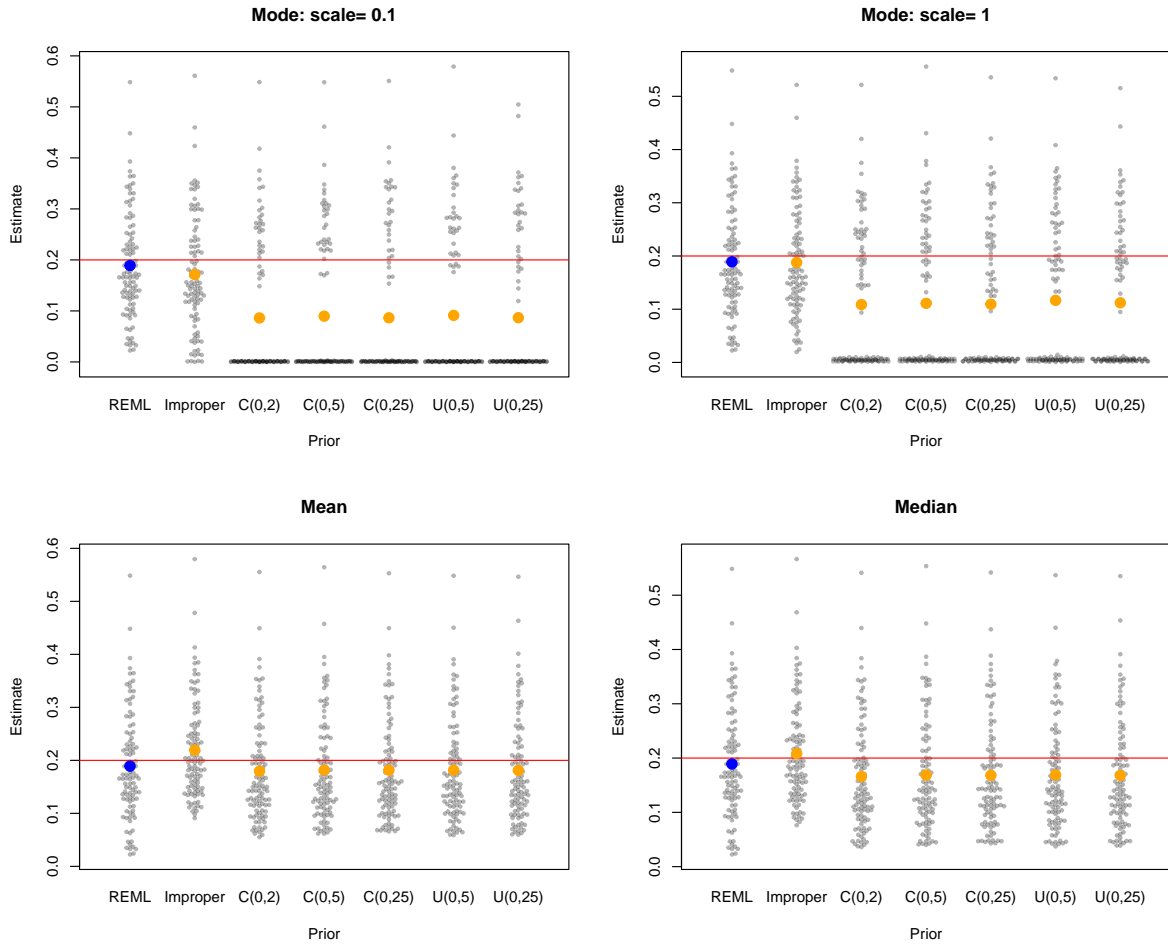


Figure S2: Impact of prior choice on measures of central tendency. 'C' represents half Cauchy priors, 'U' uniform priors, and 'Improper' uninformative improper prior. Red lines shows simulated values, and orange points shows means of different point estimates from across simulations, and blue points show the mean of the REML estimates across simulations.

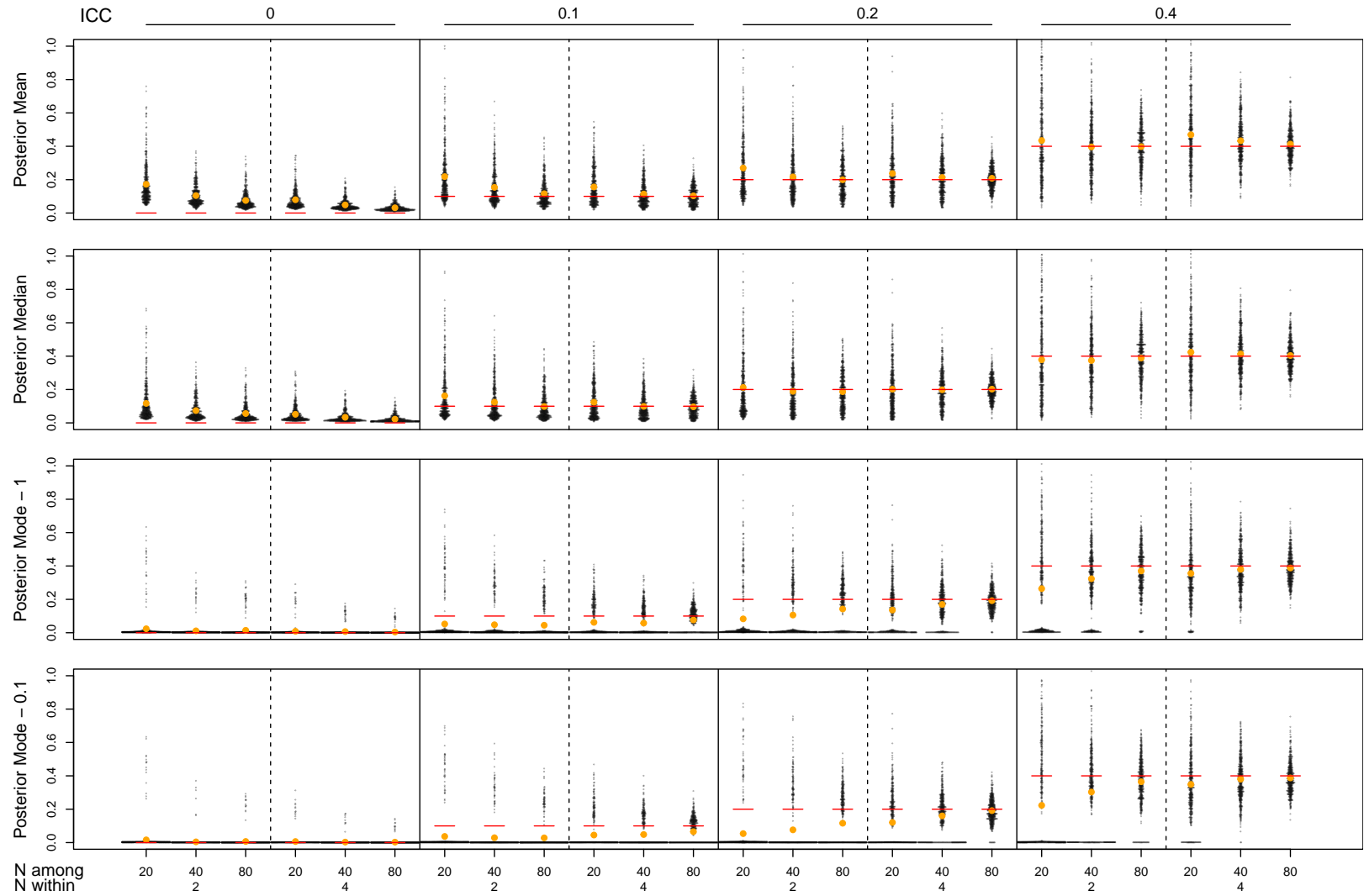


Figure S3: Sampling distributions of posterior mean, median and mode from simulations varying in among-group variance (ICC - 0, 0.1, 0.2, and 0.4) and sample size within (2 or 4) and among (20, 40, 80) groups. Red lines show the simulated value and orange points the mean of the sampling distributions.

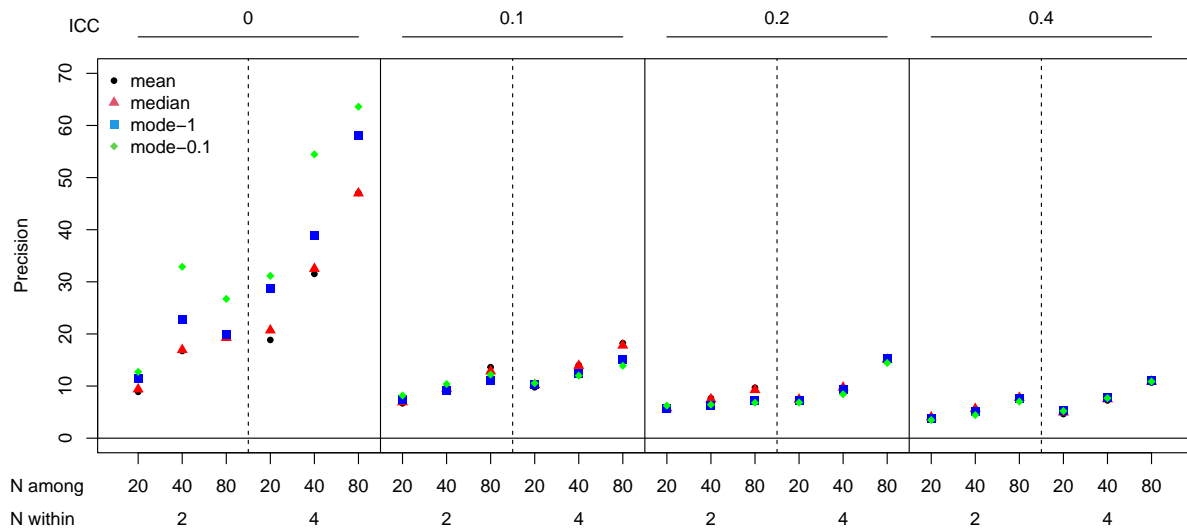


Figure S4: Precision increases with sample size, but decreases with effect size. The different panels show the precision of posterior mean, median and mode of variance components from simulations varying in among-group variance (ICC - 0, 0.1, 0.2, and 0.4) and sample size within (2 or 4) and among (20, 40, 80) groups. Two posterior modes were estimated; mode-1 and mode-0.1 with more and less smoothing, respectively (see text for more details).

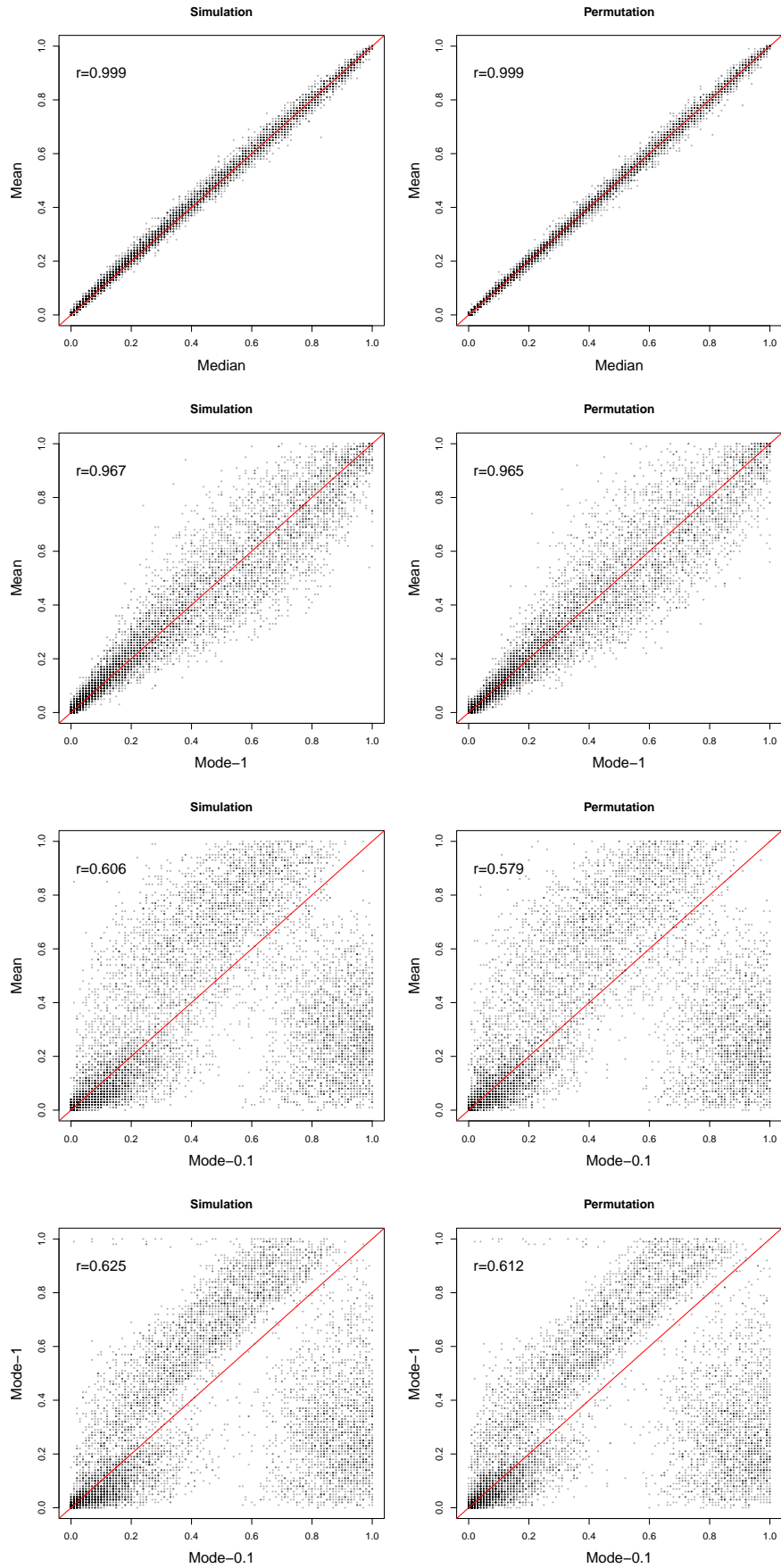


Figure S5: Comparison of p-values generated with different measures of central tendency using both simulations and permutations.

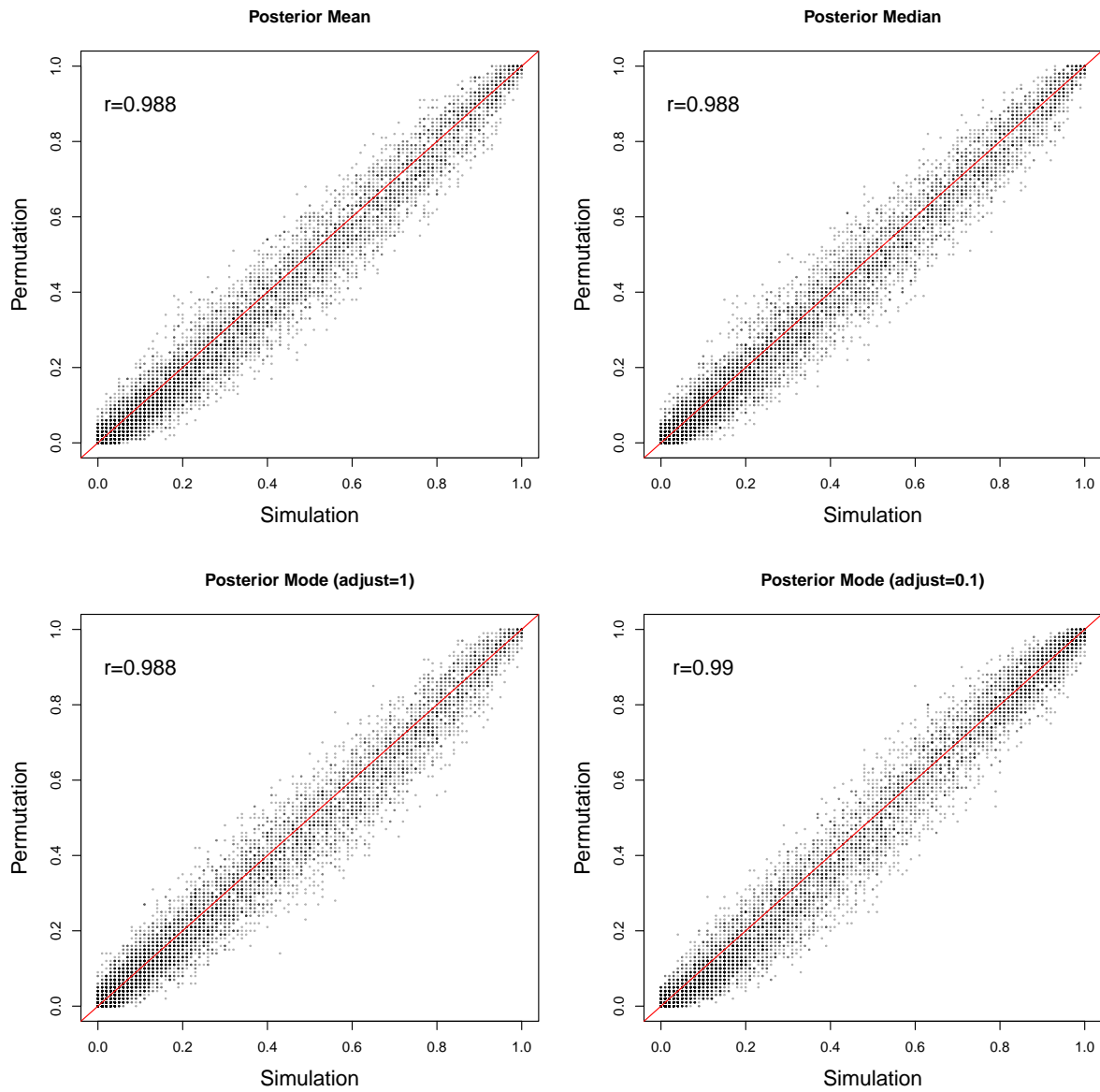


Figure S6: Comparison of p-values generated using permutation and simulation methods across all measures of central tendency.

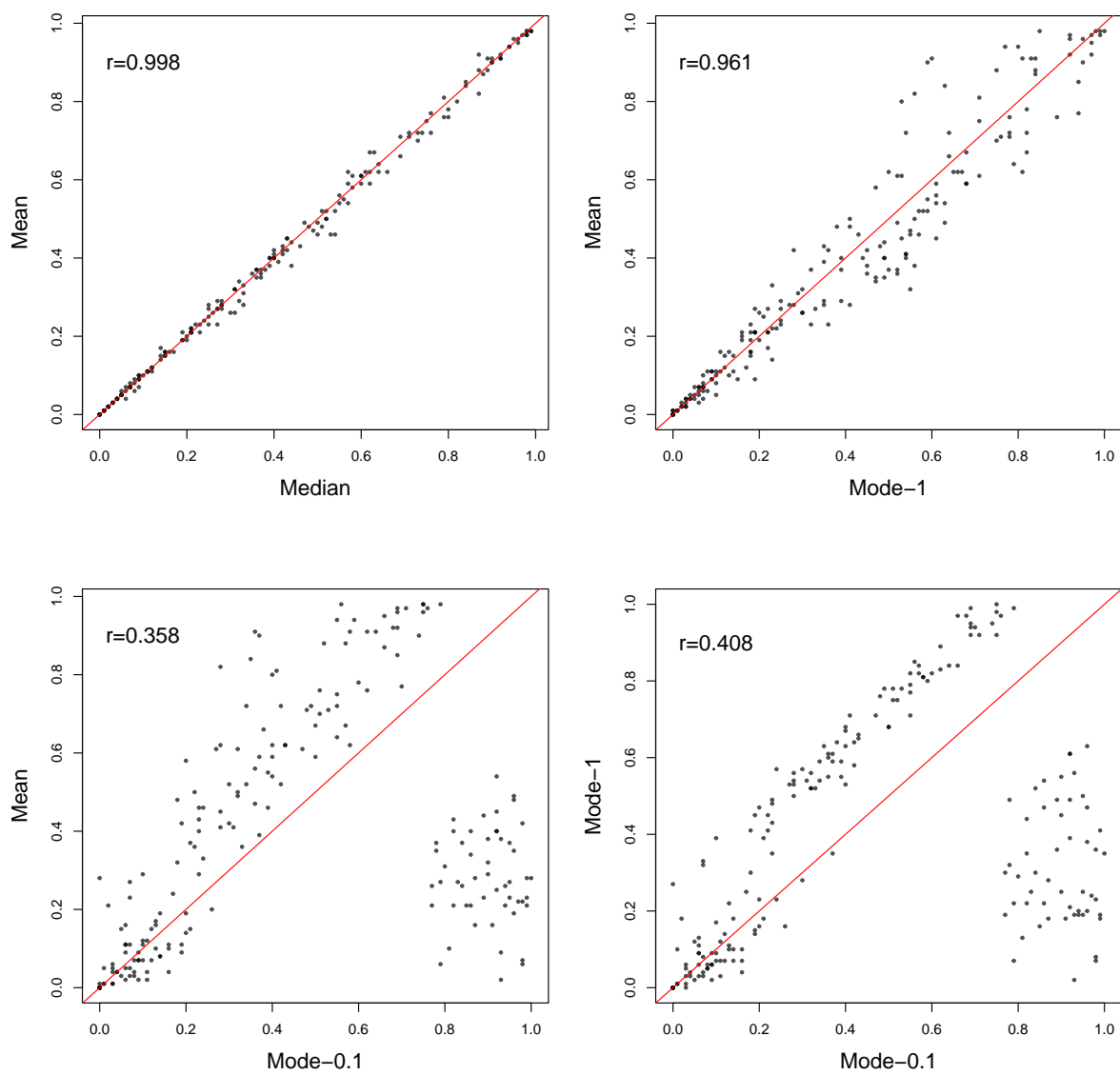


Figure S7: Comparison of p-values generated with different measures of central tendency from GLMMs using null distributions generated by simulation.

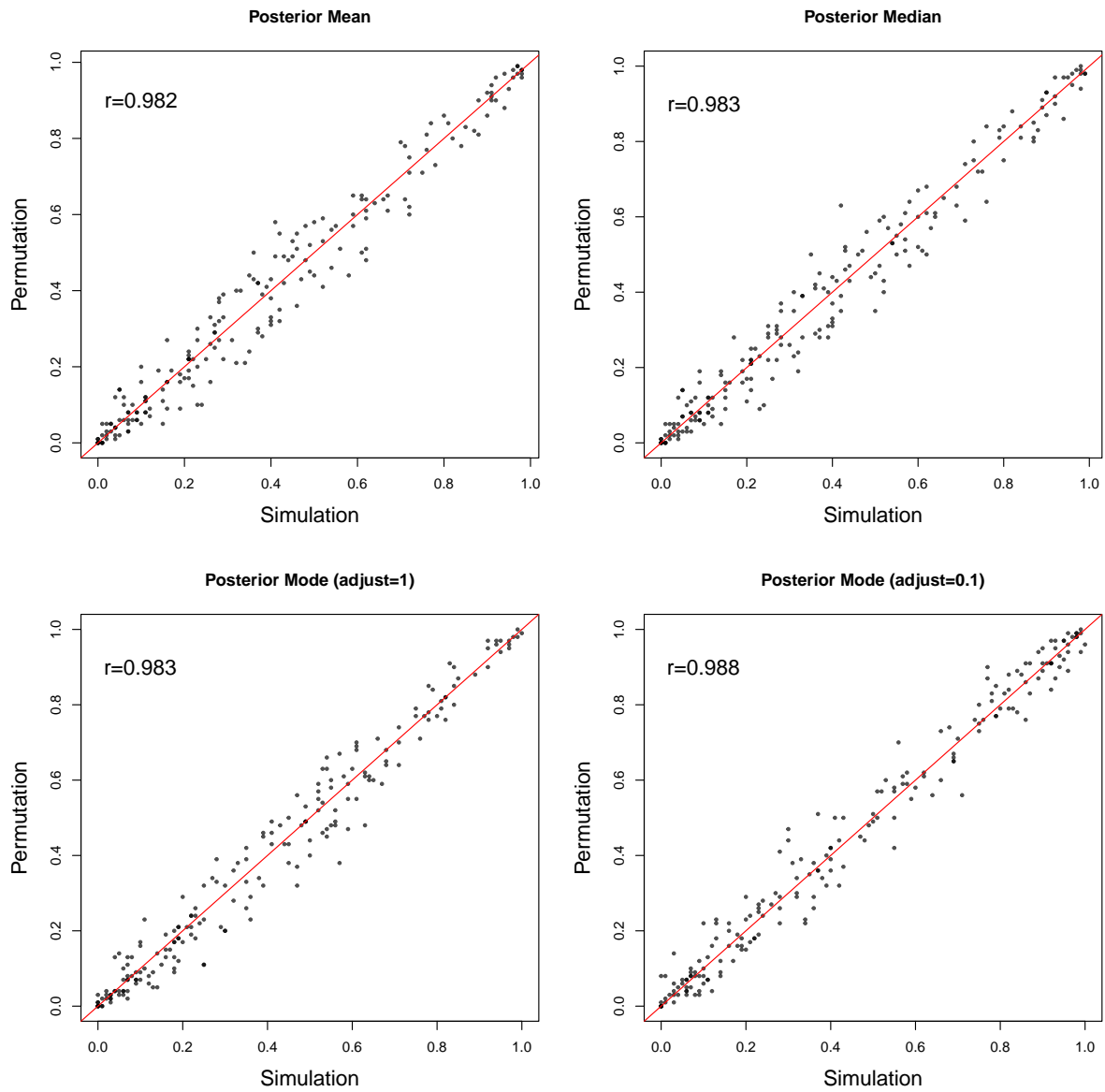


Figure S8: Comparison of p-values from GLMMs generated using permutation and simulation methods across all measures of central tendency.

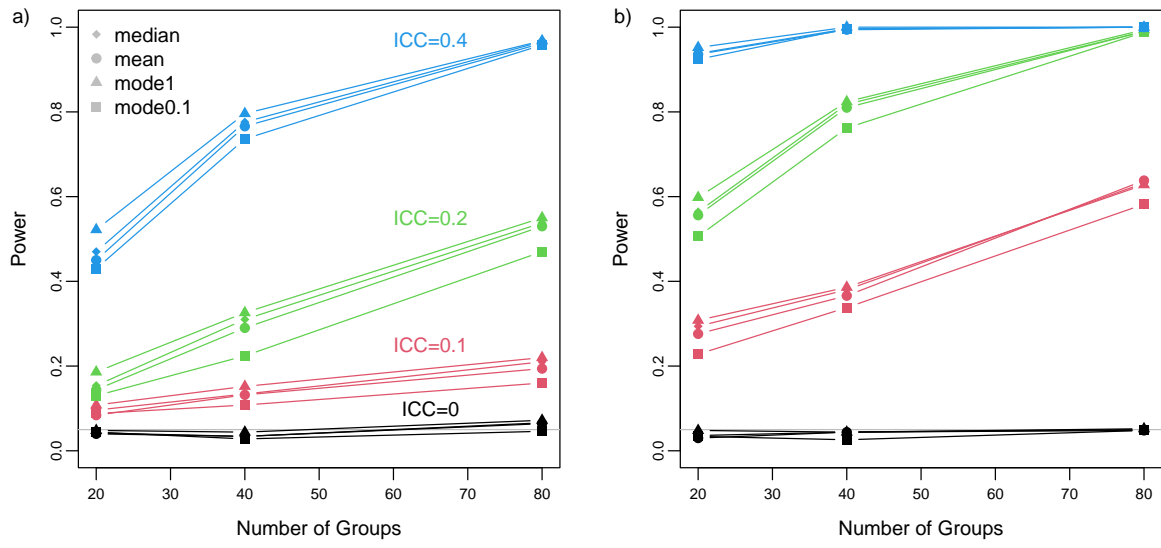


Figure S9: Comparison of power among different measures of central tendency

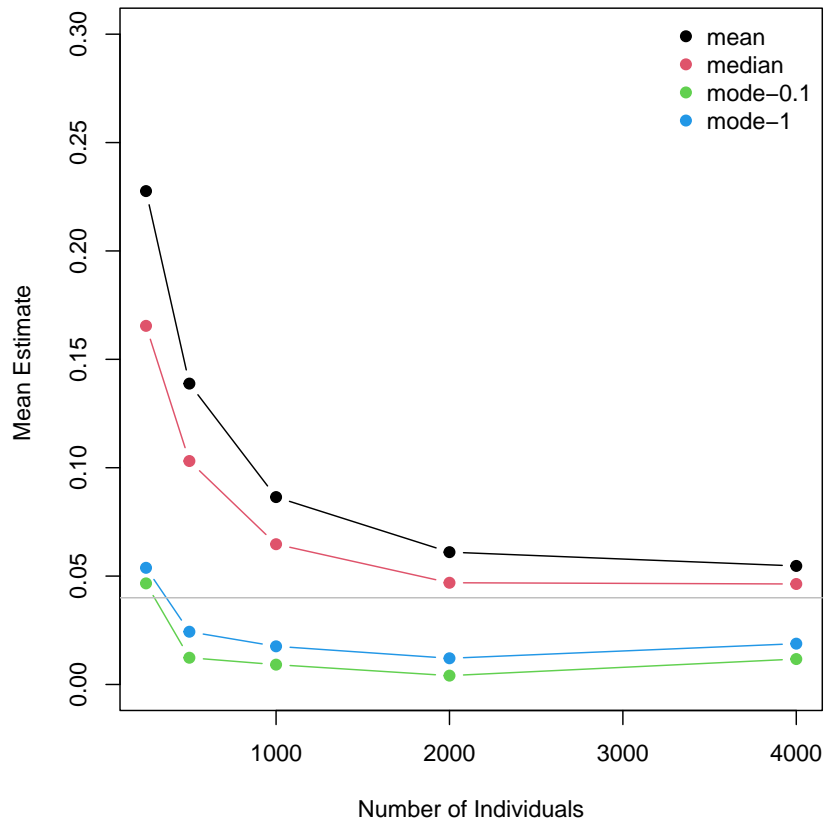


Figure S10: Mean posterior mean, median and mode of variance components from simulations based upon [Fay et al. \(2022\)](#).

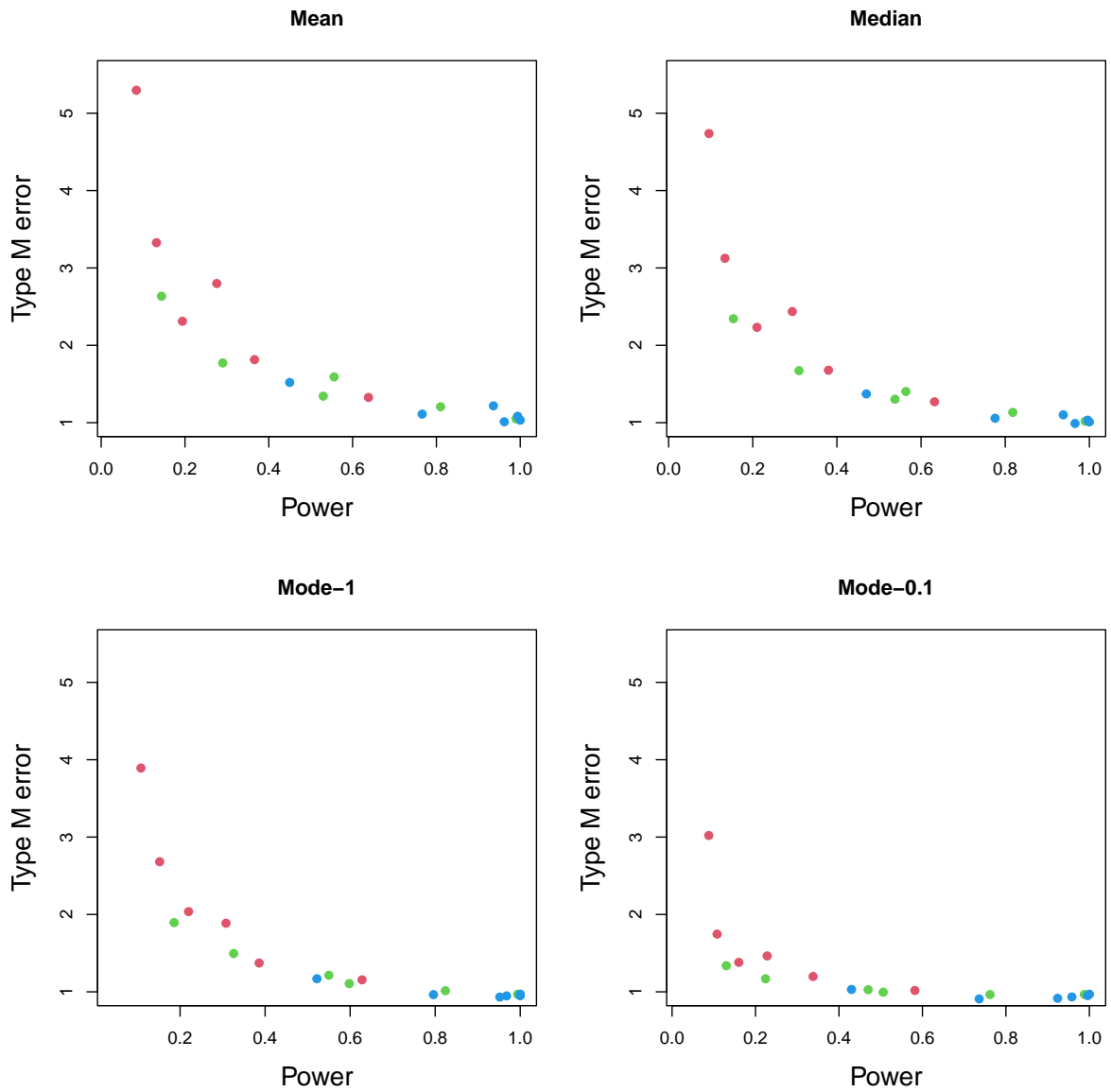


Figure S11: Type M error and power from posterior mean, median and mode calculated using null distribution generated through simulation. Colours represent simulated ICCs, red - 0.1, green - 0.2, and blue - 0.4.